JOURNAL OF GEOPHYSICAL RESEARCH, VOL. 96, NO. B10, PAGES 16,547–16,565, SEPTEMBER 10, 1991

Application of the Global Positioning System to Crustal Deformation Measurement 1. Precision and Accuracy

KRISTINE M. LARSON

Colorado Center for Astrodynamics Research, University of Colorado, Boulder

DUNCAN C. AGNEW

Institute of Geophysics and Planetary Physics, Scripps Institution of Oceanography, La Jolla, California

In this paper we assess the precision and accuracy of interstation vectors determined using the Global Positioning System (GPS) satellites. These vectors were between stations in California separated by 50-450 km. Using data from tracking the seven block I satellites in campaigns from 1986 through 1989, we examine the precision of GPS measurements over time scales of a several days and a few years. We characterize GPS precision by constant and length dependent terms. The north-south component of the interstation vectors has a short-term precision of 1.9 mm + 0.6 parts in 10^8; the east-west component shows a similar precision at the shortest distances, 2.1 mm, with a larger length dependence, 1.3 parts in 10^8. The vertical precision has a mean value of 17 mm, with no clear length dependence. For long-term precision, we examine interstation vectors measured over a period of 2.2 to 2.7 years. When we include the recent results of Davis et al. (1989) for distances less than 50 km, we can describe long-term GPS precision for baselines less than 450 km in length as 3.4 mm + 1.2 parts in 10^8, 5.2 mm + 2.8 parts in 10^8, 11.7 mm + 13 parts in 10^8 in the north- south, east-west, and vertical components. Accuracy has been determined by comparing GPS baseline estimates with those derived from very long baseline interferometry (VLBI). A comparison of eight interstation vectors shows differences ranging from 5 to 30 mm between the mean GPS and mean VLBI estimates in the horizontal components and less than 80 mm in the vertical. A large portion of the horizontal differences can be explained by local survey errors at two sites in California. A comparison which suffers less from such errors is between the rates of change of the baselines. The horizontal rates estimated from over 4 years of VLBI data agree with those determined with 1-2 years of GPS data to within one standard deviation. In the vertical, both GPS and VLBI find insignificant vertical motion.

INTRODUCTION

Many geodetic techniques have been used to measure crustal deformation across the North American/Pacific plate boundary in California. The oldest data come from triangulation measurements [e.g., *Hayford and Baldwin*, 1908]; more recently, precise electronic distance measurement (EDM) has provided many details about strain across faults of the plate boundary [e.g., *Savage*, 1983]. Both of these procedures measure through the atmosphere and require the measurement points to be intervisible; they are thus limited to distances up to a few tens of kilometers. Both require considerable skill and expensive equipment to pursue successfully.

In the past decade, measurements using extraterrestrial objects, such as satellite laser ranging (SLR) [*Christodoulidis et al.*, 1990; *Smith et al.*, 1990] and very long baseline interferometry (VLBI) [*Herring et al.*, 1986; *Clark et al.*, 1987], have made possible measurements between points hundreds to thousands of kilometers apart. This has enabled a direct determination of the total contemporary plate motion across the broad boundary in California. These observations are, however, even more expensive to make than the older, purely terrestrial, techniques.

The most recent advance in precise geodetic measurements has been the use of the Global Positioning System (GPS) satellites. The basic principles of this technique are similar to VLBI, with some important differences. The radio signals originate at satellites, rather than quasars, and GPS receivers make an instantaneous determination of the distance between the receiver and satellite, rather than requiring cross correlation of noise signals to determine the length between two sites. From enough measurements of signals arriving from different directions the complete vector baseline between two sites can be computed. Because the signal strength at the Earth is so much higher than for the quasar sources used in VLBI and because the signal has a known and well-controlled structure, GPS antennas (and all other equipment) weigh at most a few hundred pounds rather than the many tons needed for VLBI. A similar favorable ratio applies to the costs of the two techniques. For all these reasons, GPS is poised to become the method of choice for crustal deformation geodesy and in many areas has indeed already become so.

But since this is such a new technique, it is vital to establish just what its errors are. Judging from past experience with VLBI and SLR, constructing a formal error budget, while useful, is likely to give an incomplete picture because of the wide variety of semisystematic errors that are little understood (not to mention those that are overlooked). We feel that what is needed is an empirical investigation of the precision and accuracy of GPS measurements, judged from actual results: the precision being a measure of how exact the estimate is, and the accuracy a measure of how close the estimate is to the truth [*Bevington*, 1969]. Our measure of

Paper number 91JB01275.
0148–0227/91/91-JB-01275$05.00

precision is thus (as for others) the scatter of results about a mean value; our measure of accuracy is the agreement with some other technique (VLBI).

This paper is the first of three that describe results from nearly three years of measurements in central and southern California. This paper describes the precision and accuracy over baselines from 50-450 km. Though some earlier work [e.g., *Dong and Bock*, 1989] has demonstrated subcentimeter precision over these distances, this precision was only evaluated from data collected over a few days. Such estimates are likely to underestimate the long-term precision because a number of error sources probably do not change much over this span of time. The only paper that has looked at long-term precision and accuracy is that of *Davis et al.* [1989], but most of the data shown there were for baselines of 200 m to 50 km, not the longer regional scales we discuss here. This suite of measurements also allows us to discuss the role of orbit determination (fiducial) networks in establishing a consistent reference frame [*Larson et al.*, this issue] (hereafter referred to as paper 2), and the effect of different modeling procedures for the atmospheric delay (K.M. Larson and J.L. Davis, manuscript in preparation; hereinafter referred to as paper 3). In the next section of this paper, we describe how the GPS data were collected and the analysis techniques we used to determine the coordinates of the different stations. The following sections discuss precision and accuracy.

Experimental Procedure and Data Analysis

The data we use were collected during 11 "experiments" conducted between June 1986 and March 1989. The measurements in southern and central California were made by a four-university consortium, Scripps Institution of Oceanography, California Insitute of Technology, University of California, Los Angeles, and Massachusettes Institute of Technology, with substantial help from the U.S. Geological Survey (USGS) and the National Geodetic Survey (NGS). When possible, we also included data from the North American network of fixed GPS trackers that are part of the Cooperative International GPS NETwork (CIGNET) [*Chin*, 1988]. Table 1 lists 22 of the GPS sites observed. The stations located in California are shown in Figure 1. The remaining sites, all located in North America, were used for precise orbit determination, and are discussed in paper 2. While more sites than these were observed during the 11 experiments, only these 22 were measured at more than one epoch and thus can provide a useful estimate of long-term precision and accuracy. As noted above, the network formed by those of the stations in California yields baseline lengths from 50 to 450 km.

In each experiment the GPS satellites were tracked at each station using a TI-4100 dual-frequency receiver [*Henson et al.*, 1985], recording both carrier phase and pseudorange data at 30-s intervals. (Carrier phase is precise but ambiguous by an integer number of cycles; pseudorange is unambiguous but 2 orders of magnitude less precise.) The intention was to track for the 7-8 hours that several satellites were visible; for most of the experiments (all but those done in May, June, and September) this meant tracking almost entirely at night. For most experiments the plan was to record data for 4 or 5 consecutive days, a goal not always achieved in practice. Table 2 summarizes the data available from all the sites we have considered. The receiver antenna was centered over the geodetic monument at each site using an optical plummet, with a nominal accuracy of about 1 mm; the vertical offset between the antenna and the top of the monument was measured by a tape, with perhaps 2-

TABLE 1. GPS Stations

	Station	Location	Longitude, deg	Latitude, deg	Height, m	Stamping
1,	Algonquin	Ontario, Canada	-78.071	45.958	209	TELESCOPE REF A
2,	Blancas	Monterey	-121.284	35.666	50	none
3,	Blackhill	Morro Bay	-120.831	35.360	201	BLACKHILL 1881
4,	Brush	Catalina Isl.	-118.404	33.409	451	BRUSH 1976
5,	Buttonwillow	Bakersfield	-119.394	35.405	64	A364 1953
6,	Center	Santa Cruz Island	-119.753	33.996	394	CENTER 1934
7,	Churchill	Manitoba, Canada	-94.088	58.758	31	GEOS3
8,	Clembluf	San Clemente Island	-118.518	32.928	297	BLUFF 1933
9,	Fort Ord	Monterey	-121.773	36.671	39	FORT ORD NCMN 1981
10,	Lacumbre	Santa Barbara County	-119.713	34.496	1171	none
11,	Lospe	Vandenberg AFB	-120.605	34.896	505	none
12,	Madre	Miranda Pine Mountain	-120.067	35.077	914	MADRE ECC 1980
13,	Mojave	Goldstone	-116.888	35.333	904	CIGNET
14,	Niguel	Laguna Niguel	-117.730	33.516	238	NIGUEL A 1884 1981
15,	Nicholas	San Nicolas Island	-119.479	33.233	201	TWIN 1964
16,	OVRO	Owens Valley	-118.293	37.234	1195	MOBLAS 7114 1979
17,	Palos Verdes	Los Angeles	-118.403	33.745	73	PALOS VERDES ARIES 1976 1980
18,	Platteville	Colorado	-104.726	40.184	1530	PLATTEVILLE NCMN 1981
19,	Richmond	Florida	-80.384	25.615	23	CIGNET
20,	Soledad	La Jolla	-117.252	32.841	216	none
21,	Vandenberg	Vandenberg AFB	-120.616	34.558	24	VLBI STA 7223 RM1
22,	Westford	Haystack Obs., Mass.	-71.493	42.615	125	CIGNET

Geodetic coordinates of crustal deformation sites, referenced to NAD 83. The stamping is imprinted on the geodetic marker. CIGNET refers to the antenna phase center of the continuously monitoring GPS network [*Chin*, 1988]. Unless otherwise noted, all sites are in California.

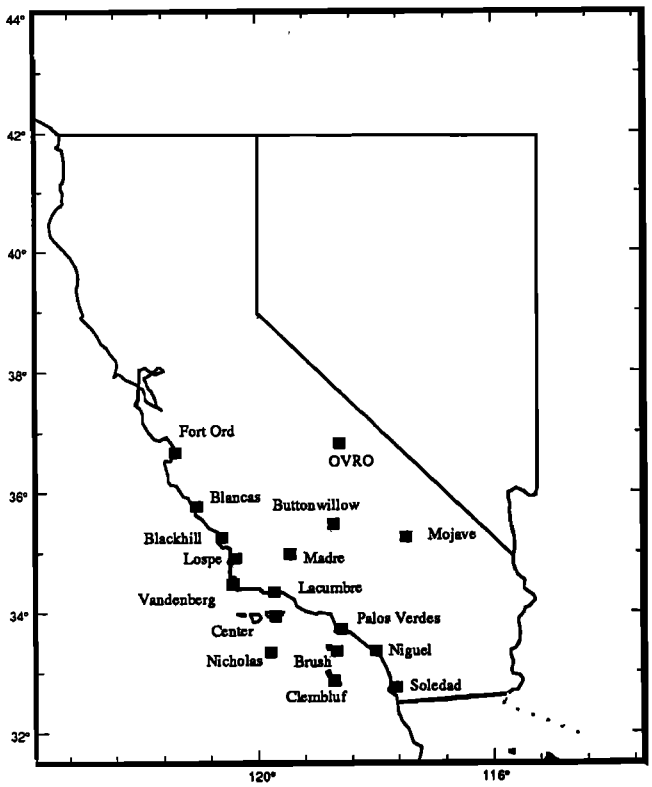

Fig. 1. GPS sites in southern and central California observed between 1986 and 1989 for crustal deformation studies. Table 1 gives the site names and coordinates, and Table 2 gives a breakdown of which sites were observed when. All but three (Mojave, Buttonwillow, and OVRO) lie west of the San Andreas fault.

mm error. While the observers at each site recorded local pressure, temperature, and humidity, we have not made use of these data (paper 3 discusses this in more detail).

The GPS data were analyzed with the GPS Inferred Positioning SYstem software (GIPSY) developed at the Jet Propulsion Laboratory [*Stephens*, 1986; *Lichten and Border*, 1987]. GPS carrier phase and pseudorange data at both frequencies were reformatted from the original data tapes, and the phase data were checked for cycle slips. This process was automated by using a computer program, Turboedit, described by *Blewitt* [1990]. In order to reduce the computer storage and CPU requirements, we subtracted a model of satellite and station positions from the observables, and a second order polynomial fit was used to compress the 30-s data to 6-min points. This technique is valid as long as the error sources over 6 min (satellite and receiver clocks and the ionosphere) can be modeled by a second-order polynomial. At this point, linear combinations were formed of the carrier phase and pseudorange data, which eliminated the highest-order effects of the ionosphere. Nominal satellite trajectories were determined by a module which integrates the equations of motion and the variational equations to obtain satellite coordinates and partial derivatives of these coordinates with respect to the satellite initial conditions and force parameters. Another module computed prefit residuals and partial derivatives from nominal station coordinates, nominal GPS orbits, and models for the Earth's rotation, tides, and atmospheric refraction [*Sovers and Border*, 1988]. Finally, a factorized Kalman filter was used to perform a least squares adjustment of station positions, satellite initial positions and velocities, tropospheric zenith delays, phase ambiguities, and satellite and receiver clocks.

The constraints we used for our standard estimation procedure are summarized in Table 3. We used the broadcast ephemeris to determine nominal values for initial position and velocity of each spacecraft. For each satellite, we estimated an initial position, initial velocity, and the behavior of the satellite clock. We fixed the positions of three "fiducial sites", whose coordinates were derived from VLBI measurements. If properly chosen, these fiducial sites, whose positions are known to better than 2 cm, provide sufficient strength to determine the satellite orbit to better than 2 m (see paper 2 for further detail on both the derivation of fiducial coordinates and their impact on orbit determination). If more than three "VLBI sites" were included in a GPS experiment, the nonfiducial VLBI sites were treated as "mobile sites" and estimated with a standard deviation of 2 km. In general, our starting (nominal) solution was within 1 m of the estimated position of all mobile stations.

We modeled the clock bias at each measurement point as white noise; in other words, each estimate was independent and uncorrelated with the clock bias at previous measurements. Some receivers we used were connected to hydrogen masers; the remainder used the quartz internal clock provided by the TI-4100. White noise clock modelling is essentially identical to the double differencing used in other softwares [*Beutler et al.*, 1990].

The optimal strategy for determining the atmospheric propagation delay is unclear at this time. *Tralli et al.* [1988] suggest time-varying estimation techniques are preferable, while *Davis et al.* [1989] achieve similar vertical component precision solving for a constant zenith delay parameter. Water vapor radiometers (WVR) were not in use during 10 of the 11 experiments, and therefore we have chosen to ignore what little WVR data were available. Paper 3 will address this issue in more detail. The strategy we have used in this paper was as follows: we first corrected for the dry troposphere delay using a crude relation between station elevation, pressure, and dry zenith delay. The pressures for hydrostatic zenith delay calculations were determined using the ellipsoidal height of the site and an assumed sea level pressure of 1013.24 mbar with an exponential profile with scale height 7 km. The temporal variation of the wet zenith path delay was modeled as a random walk, with an allowed variation of 49 mm over 7.5 hours.

Finally, a station-satellite parameter was estimated for each phase ambiguity. The nominal phase ambiguity solution was determined from the pseudorange data. Subsequently, ambiguity resolution was attempted. We used a 99% confidence criterion for "fixing" these ambiguities to their integer values, which is described by *Blewitt* [1989]. At this point, postfit residuals were visually inspected, primarily to determine if cycle slips had been incorrectly fixed. At this point the Cartesian station locations and their standard deviations can be retained for crustal deformation studies.

The reference frame we used was defined by the Goddard Space Flight Center Global Site Velocity model GLB223, which is based on over 4 years of VLBI data (C. Ma, personal communication, 1988). Further discussion of the reference frame is left to paper 2. Earth orientation values were taken from the monthly bulletins of the International Radio Interferometric Surveying (IRIS) Subcommission.

TABLE 2a. Data Summary

	Experiment										
	J86[a]	D86	J87	M87[b]	S87	M88a	M88b	J88	S88	M89a[c]	M89b
Month/year	June 1986	Dec. 1986	Jan. 1987	May 1987	Sept. 1987	March 1988	March 1988	June 1988	Sept. 1988	March 1989	March 1989
Dates	17-20	12/30-1/2	27-29	25, 27, 28	22,24,25	8,9,11	15-18	8-11	13-16	21-23	28-30
Total days of data	4	4	3	3	3	3	4	4	4	3	3
1, Algonquin	-	4	-	-	-	-	4	-	-	-	-
2, Blancas	-	2	-	-	-	-	4	-	-	-	3
3, Blackhill	-	4	-	3	3	-	4	-	-	-	3
4, Brush	-	-	3	-	-	3	-	-	-	3	-
5, Buttonwillow	-	4	-	-	-	-	4	-	-	-	3
6, Center	-	4	3	3	3	3	4	-	-	-	3
7, Churchill[d]	-	4F	-	-	-	3F	4	-	-	-	-
8, Clembluf	2	-	3	-	-	3	-	-	-	3	-
9, Fort Ord[e]	-	4F	-	-	3F	-	4F	-	4	-	-
10, Lacumbre	-	4	3f	-	-	-	4	-	-	-	2
11, Lospe	-	1.5	-	-	-	-	3.5	-	-	-	3
12, Madre	-	4	-	-	-	-	4	-	-	-	3
13, Mojave[f]	4F	1	3F	3	2.5	3F	2.5	3F	4F	3F	3F
14, Niguel	2	-	-	-	-	2	-	-	-	3	-
15, Nicholas	4	-	-	-	-	-	4	-	-	3	-
16, OVRO	-	1.5	-	3F	3	-	3.5	-	-	-	3f
17, Palos Verdes	4	-	3f	3	3	1	4	4	4	3f	3f
18, Platteville	-	4	-	-	3F	2	3	-	-	-	-
19, Richmond[g]	4F	-	-	-	-	1F	3F	3F	2F	0	0
20, Soledad	2	-	3	-	-	3	-	-	-	3	-
21, Vandenberg	3	4	-	3	3	3	3	4	3	3f	3f
22, Westford	4F	4	0	3F	3F	3F	4F	4F	2F	0	0

Site occupations are summarized for 11 experiments at 22 sites between June 1986 and March 1989. The total days of available data are listed. Individual station occupations are listed by experiment. F, the station position was not estimated, i.e. this is a fiducial site; f, the station position was estimated, with a standard deviation of 20 mm; Number of days of useful data. One day of data equals approximately 7 hours. If no f or F is listed, station position was estimated, with a standard deviation of 2 km. Dashes indicate the station was not scheduled to be observed during the experiment. Zero indicates the station was scheduled to be observed, but no useful data were collected.

[a] Experiment described in greater detail by *Blewitt* [1989]

[b] Austin, Texas used as third fiducial site. Coordinates provided by M. Murray (personal communication, 1990)

[c] Less than 10% of carrier phase ambiguities were resolved between sites in California.

[d] Fiducial coordinates for Churchill determined from data collected during experiment M88b

[e] Fort Ord was destroyed summer of 1988. Reference mark was occupied in S88

[f] Mojave refers to 3 "monuments". J86 = Mojave NCMN1; D86-J88 = CIGNET TI-4100 antenna; S88-M89b = CIGNET FRPA antenna. Mini-MAC data collected at Mojave for M89a and M89b were not used.

[g] CIGNET tracker at Richmond was unavailable until November 1988

TABLE 3. Parameter Estimation

Parameter	Estimation	Standard Deviation	Steady State Standard Deviation	Time Behavior
Satellite position, km	force model	100		
Satellite velocity, km/s	force model	1		
Satellite clock, s	stochastic	1	1	white noise
Station position (fiducial)	fixed (not estimated)			
Station position (mobile), km	constant	2		
Station clock, s	stochastic	1	1	white noise
Phase ambiguity, s	constant	10		
Zenith troposphere delay	stochastic	300 mm	3×10^{-7} km/$\sqrt{s}$	random walk
Data weights, mm	pseudorange	250		
	carrier phase	10		

PRECISION

Introduction

To characterize the precision of the vectors estimated by GPS, we use the scatter of independently estimated results. For short-term precision, we will use results from 18 stations observed during a single experiment in March 1988. Short-term precision will be defined by the weighted RMS scatter about the mean of daily estimates, each determined from a single-day orbit solution. If we have N independent values $y_1, y_2, \ldots y_N$ with (formal) standard errors $\sigma_1, \sigma_2, \ldots \sigma_N$, this scatter is S_{mean},

$$S_{mean} = \sqrt{\frac{\frac{N}{N-1}\sum_{i=1}^{N}\frac{(y_i - \langle y \rangle)^2}{\sigma_i^2}}{\sum_{i=1}^{N}\sigma_i^2}} \quad (1)$$

where $\langle y \rangle$ is the weighted mean of the y_i's. (This quantity has sometimes been termed the repeatability, a term we eschew because it leads to ambiguity: a high repeatability may be highly repeatable (good), or a large value (bad).) The reduced χ^2 statistic is defined for the weighted RMS about the mean as

$$\chi^2_{mean} = \frac{1}{N-1}\sum_{i=1}^{N}\frac{(y_i - \langle y \rangle)^2}{\sigma_i^2} \quad (2)$$

where y_i, σ_i, and $\langle y \rangle$ are defined as before. A reduced χ^2 of 1 indicates that the formal errors, σ_i, agree with the actual scatter in the measurements.

Since our measure of precision is weighted by our expected error, we need to describe how these formal errors were calculated. The measurement standard deviation is calculated by propagating standard deviations of the carrier phase and pseudorange data through the variance-covariance matrix. Our formal errors then are dependent on the data weights we assumed for the carrier phase and pseudorange data, 10 and 250 mm, respectively. These data weights were determined empirically in the following manner. For each station, we multiplied the RMS post-fit scatter by the quantity $\sqrt{N/(N-P)}$, where N is the number of data points and P is the number of parameters we have estimated. This data noise is then approximately what is required to make χ^2 one. In general, the RMS postfit scatter ranged from 4 to 6 mm, depending on the station, and the scaling quantity was approximately 1.5. This resulted in a data weight of 6-9 mm. In an effort to be conservative, we chose 10 mm and applied it uniformly to all stations. We determined the pseudorange data weight in the same manner. This data weight would have to be changed if we substantially increased the number of parameters we estimated, or we changed the data rate (i.e., from 6 to 3 min points). For the experiments listed in Table 2, we had fairly common data sets, in numbers of satellites, and we used consistent estimation procedures. Thus, while our formal errors may be incorrect, they were computed in an identical fashion for each experiment. Later in this section we will discuss whether our weighting scheme was appropriate.

We expect that short-term precision might underestimate the true precision, because over this time scale some errors change less than they would over longer times. Possible errors in this class are wet and dry tropospheric delays and set-up errors. To estimate long-term precison we use measurements spanning 1.2-2.7 years for 22 stations (including all those used for the short-term precision estimates). We could use equation (1) for long-term precision, but by neglecting actual plate motion we unnecessarily degrade the precision of the GPS estimate. Therefore, for long-term horizontal precision, we adopt a standard technique [*Ma et al.*, 1990] and calculate the weighted RMS about the best fitting line. (For long-term vertical precision, we assume no true vertical motion, and use equation (1) only.) The weighted RMS about the best fitting line, S_{line}, is defined

$$S_{line} = \sqrt{\frac{\frac{N}{N-2}\sum_{i=1}^{N}\frac{(y_i - (a + bt_i))^2}{\sigma_i^2}}{\sum_{i=1}^{N}\sigma_i^2}} \quad (3)$$

where a and b are the intercept and slope of the best fitting line and t_i is the time of the ith measurement. The reduced χ^2 statistic for S_{line} is

$$\chi^2_{line} = \frac{1}{N-2}\sum_{i=1}^{N}\frac{(y_i - (a + bt_i))^2}{\sigma_i^2} \quad (4)$$

These formulae are correct if we can assume that each es-

timate of an interstation vector is independent. In general, our data were collected several days in succession, separated by 6-12 months, and thus were not evenly distributed in time. Even though we have analyzed each day of GPS data independently, *Davis et al.* [1989] have pointed out that estimates only a few days apart will be correlated, due to common error sources. Therefore, Davis et al. attempted to separate short- and long-term error statistics. The short-term error was determined by the scatter about the mean for a single 3-5 day experiment, and the long-term error was computed from the RMS of these means about the best fitting line. The total error was then computed assuming the long- and short-term errors were independent. One problem with this formulation is that it ignores the formal errors, with all estimates being treated equally. When we used the Davis et al. technique, we found that measurements from the M89a and M89b experiments were the largest contributors to the long-term error. We know there were systematic errors in that particular experiment, caused by the fiducial network we were forced to use. Since this paper is a summary of a large quantity of data, we would like to leave discussion of known systematic errors to papers 2 and 3. If one adapts the method of Davis et al. to incorporate the formal errors, one is then computing nearly the same quantity as if equation (3) were used. We therefore use the simplest formulation we have for long-term precision, equation (3), although we recognize that we have not solved for the long- versus short-term error sources.

While much of the information about precision is best obtained from the plots of scatter, we also wish to summarize the results in a compact way. One way of summarizing errors of distance measurements is the expression [*Savage*, 1983]

$$\sigma^2 = A^2 + B^2 l^2 \tag{5}$$

where σ is the standard deviation and l is the baseline length. This equation derives from the nature of EDM measurements [*Rueger*, 1990], where the measuring instrument has a constant error A, a proportional error B being introduced by errors in the estimated atmospheric refraction. Equation (5) then follows from the usual law for the combination of independent errors.

The dependence of error on distance might be expected to be more complicated for GPS measurements. Over very short baselines (<100 m) the intrinsic precision and accuracy of the measurement are 2 mm or less [*Davis et al.*, 1989], though in many survey conditions we might expect the errors of locating the antenna relative to the geodetic monument to be several times this. Another source of error that is independent of length is the effect of antenna multipath: the signal received is the sum of the direct-arriving radio wave and waves that have been reflected off nearby objects (such as the ground). As the position in the sky of a satellite changes the relative contributions of these waves will vary, causing the apparent location of the antenna to wander about its true one. Because of the long duration of tracking during these measurements we expect this error to be small.

Over longer distances other error sources enter in. For distances of more than the troposphere scale height (a few kilometers), differences in wet and dry delay cease to cancel, at least relative to other error sources; at larger distances the same becomes true for the ionosphere. One well-understood error scales with baseline length: errors in the estimated orbits of the satellites. This contributes to an error in baseline

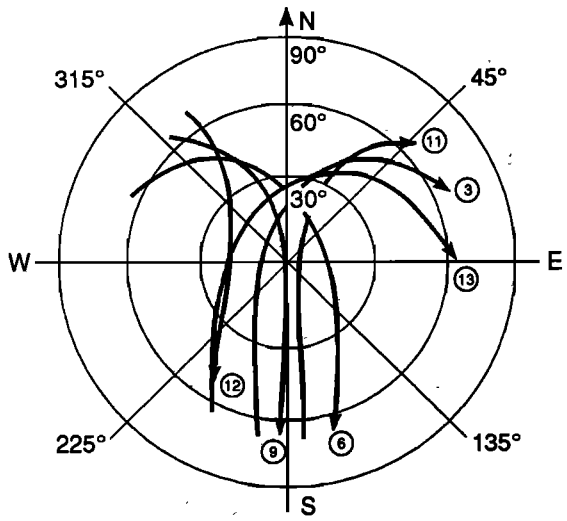

Fig. 2. GPS sky tracks over California for the six block I GPS satellites observed during the December 1986 campaign (modified from *Dong and Bock*[1989]). The anisotropy of these sky tracks gives measurements of north-south components greater inherent precision than those of east-west components.

length which is about $l\beta\sigma_{orb}/L$, where L is the distance from the GPS receiver to GPS satellites (about 20,000 km), σ_{orb} is the orbit error, and β is a constant that depends on network geometry; it is about 0.2 for continental scale networks [*Lichten*, 1990]. The GPS constellation observed during the experiments used here consisted of seven block I satellites. Figure 2 shows the sky paths of six of these satellites as seen from California; since the satellites cover a wider range of elevations along a north-south azimuth than to the east or west, we might expect the baseline error to be larger for east-west components than north-south ones. Similarly, because the data come only from satellites above the horizon, the vertical component precision can be expected to be much worse than either horizontal precision.

Because of the varied nature of errors in GPS baselines, there seems to be no good reason to adopt the form of equation (5) for the errors. However, some acknowledgment of the existence of proportional errors is appropriate; we have therefore adopted the simple law

$$\sigma = A + Bl \tag{6}$$

to summarize the change of precision with distance. We do not believe this relation truly reflects the underlying error structure of GPS; instead we use this relation as a means of summarizing the precision estimates we have made. Since our analysis is restricted to baselines from 50 to 450 km in length, we will incorporate the long-term precision results of *Davis et al.* [1989] for baselines less than 50 km in order to extend this assessment of GPS precision. Further studies will be required to determine the long-term precision of continental- and global-scale interstations vectors measured with GPS. At that time, it will be appropriate to investigate in a more systematic fashion whether equation (5), (6), or a more complicated expression adequately describes long-term precision.

Results

Short-term precision. The most successful experiment of the 11 listed in Table 2, in terms of high data yield, was the March 1988 central California campaign (designated M88b).

Four days of data were collected at 18 sites in North America, 13 in California. The short-term precision for the north-south, east-west, and vertical components for this experiment is plotted, as a function of baseline length, in Figures 3*a*-3*c* and is listed in Table 4.

The most prominent feature of these plots is the absence of significant baseline dependence for the north-south component. This has errors of 1.9+0.6 parts in 10^8. In the east-west component, the precision is described by 2.1 mm+1.3 parts in 10^8. The constant term for both components is in good agreement with the precision of 100-m baselines [*Davis et al.*, 1989]. The difference in baseline dependence for the two components is easily explained by the satellite geometry of the block I constellation discussed in the previous section. This is a similar network to the one studied by *Dong and Bock* [1989]. By fitting a line to their baseline scatter, Dong and Bock reported precision of 6 mm + 0.5 parts in 10^8 in the east-west component and 2.5 mm + 0.9 parts in 10^8 in the north- south component.

The vertical component is nearly an order of magnitude less precise than horizontal components. The scatter has a mean value of 17 mm, with no length dependence. Using data collected during the June 1986 southern California GPS experiment (see J86 in Table 2), *Blewitt* [1989] reported a mean RMS of 29 mm on baselines ranging from 50 to 650 km, which is in good agreement with formal errors from his analysis. Inspection of scatter plots in Blewitt's paper shows no baseline dependence. In contrast, *Dong and Bock* [1989] reported a slight dependence on baseline length for their vertical component precision, 12 mm + 6 parts in 10^8. The differences between our results and those of Dong and Bock may be due to the difference in fiducial networks we used. We leave this discussion to paper 2.

Discussion. Our primary objective is to use the scatter in the interstation vector estimates to determine GPS system precision. Another important question we address is the validity of the formal errors. It has long been recognized that formal errors underestimate the scatter in actual data. This is generally attributed to unmodeled systematic effects and to mismodeling of certain parameters. One technique commonly used to produce more reasonable errors is to scale formal errors so that the reduced χ^2 is 1 [*Clark et al.*, 1987]. In their study of GPS precision, *Davis et al.* [1989] discarded their formal errors and used an ad hoc technique, deriving a standard deviation from the actual scatter. While it is difficult to determine how the systematic errors impact on the precision, it is fairly simple to determine how representative the formal errors are of the actual scatter in the data. In other words, we compare the predicted standard deviation and the actual standard deviation.

Included with short-term precision in Figures 3*a*-3*c* are the formal error (the mean of the four single-day formal errors) as a function of baseline length. The north-south component indicates that the actual scatter is less than that predicted by the formal errors. The formal error predicts a scatter of 2.4 mm + 0.4 parts in 10^8, whereas the actual scatter is 1.9 mm + 0.6 parts in 10^8. For the east-west component, the formal error is 2.4 mm + 1.5 parts in 10^8, which is also close to the actual scatter of 2.1 mm + 1.3 parts in 10^8. For the vertical component, formal errors overpredict the scatter by a factor of 1.5. The vertical component formal errors are heavily dependent on the random walk parameterization we have chosen for the wet troposphere zenith delay. Thus, we leave discussion of vertical formal errors to

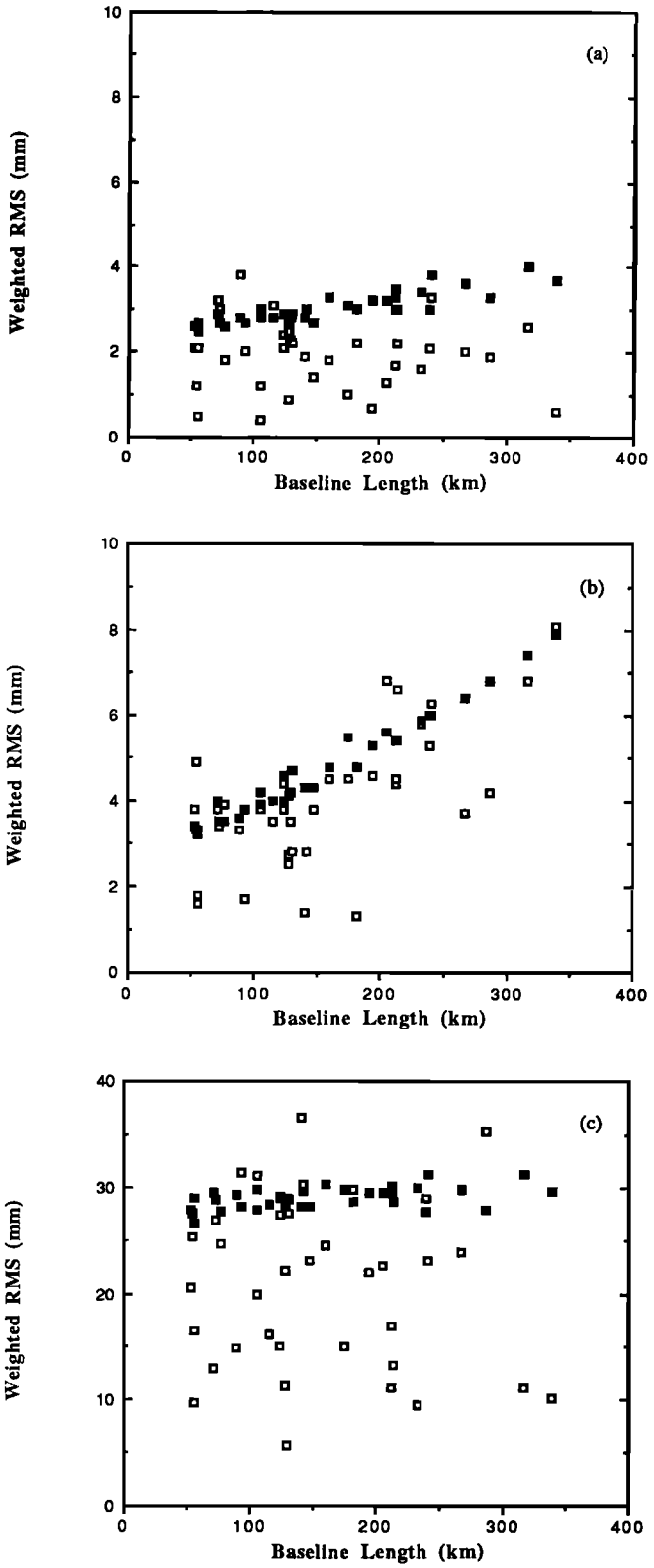

Fig. 3. The open squares are the short-term precision, defined by equation (1) as the weighted RMS about the mean, of different components of the baselines measured in March 1988, plotted as a function of line length. The solid squares are the mean of the formal 1-σ errors for the same quantities, as computed from the size of the residuals and the covariances of the least squares adjustment. Figure 3*a* is for the north-south component of the baseline; Figure 3*b* is for the east-west component, and Figure 3*c* for the vertical component. (The directions are those of a Cartesian coordinate system located at one end of the baseline, whose north is coincident with the local north, and vertical with the normal to the ellipsoid.)

TABLE 4. Short-Term Precision

Interstation Vector	Length, km	East, mm	χ^2	North, mm	χ^2	Vertical, mm	χ^2
Blackhill-Blancas	53	4.9	2.25	1.2	0.20	25.4	0.78
Lospe-Madre	53	3.8	1.29	2.1	0.68	20.6	0.52
Center-Lacumbre	55	1.6	0.22	2.1	0.64	16.4	0.33
Blackhill-Lospe	55	1.8	0.32	0.5	0.03	9.6	0.12
Buttonwillow-Madre	71	3.8	1.14	3.2	1.25	12.8	0.18
Madre-Lacumbre	72	3.4	0.96	3.0	1.13	27.0	0.82
Blackhill-Madre	76	3.9	1.25	1.8	0.46	24.7	0.73
Center-Nicholas	88	3.3	0.91	3.8	2.11	14.8	0.29
Lospe-Lacumbre	93	1.7	0.22	2.0	0.54	31.5	1.19
Buttonwillow-Lacumbre	105	4.2	1.13	0.4	0.02	31.2	1.06
Blancas-Lospe	105	3.8	1.01	1.2	0.18	19.9	0.48
Palos Verdes-Nicholas	115	3.5	0.80	3.1	1.30	16.0	0.34
Madre-Center	123	4.4	1.32	2.1	0.55	15.0	0.27
Lospe-Buttonwillow	123	3.8	0.80	2.4	0.74	27.4	0.89
Lospe-Center	127	2.7	0.52	2.5	0.86	22.2	0.64
Blancas-Madre	128	3.5	0.80	2.3	0.60	5.7	0.04
Palos Verdes-Center	128	2.5	0.43	0.9	0.11	11.3	0.18
Blackhill-Buttonwillow	131	2.8	0.45	2.2	0.60	27.6	0.88
Blackhill-Lacumbre	140	1.4	0.13	1.9	0.41	36.7	1.57
Nicholas-Lacumbre	142	2.8	0.48	3.0	1.00	30.4	1.07
Palos Verdes-Lacumbre	146	3.8	0.90	1.4	0.24	23.2	0.65
Buttonwillow-Center	160	4.5	0.98	1.8	0.31	24.6	0.70
Blancas-Buttonwillow	174	4.5	0.88	1.0	0.10	16.5	0.30
Blackhill-Center	180	1.3	0.08	2.2	0.50	29.9	1.14
Blancas-Lacumbre	193	4.6	0.95	0.7	0.05	22.0	0.52
Palos Verdes-Buttonwillow	204	6.8	2.00	1.3	0.16	22.7	0.60
Madre-Nicholas	211	4.4	0.80	3.0	0.74	11.1	0.14
Lospe-Nicholas	211	4.5	0.87	1.7	0.28	16.8	0.35
Palos Verdes-Madre	212	6.6	1.96	2.2	0.48	13.1	0.20
Blancas-Center	232	5.8	1.29	1.6	0.20	9.5	0.11
Palos Verdes-Lospe	239	5.3	1.11	2.1	0.45	29.0	1.09
Buttonwillow-Nicholas	240	6.3	1.29	3.3	0.77	23.1	0.58
Blackhill-Nicholas	267	3.7	0.44	2.0	0.31	23.9	0.67
Palos Verdes-Blackhill	286	4.2	0.55	1.9	0.32	35.3	1.53
Blancas-Nicholas	316	6.8	1.15	2.6	0.40	11.1	0.13
Palos Verdes-Blancas	339	8.1	1.60	0.6	0.02	10.2	0.12

paper 3. Comparably, plots of χ^2 as a function of baseline length, as shown in Figures 4*a*-4*c*, indicate that over the short term, the formal errors are comparable to the scatter. The outliers in the χ^2 plots, in both senses, those that are too small and those that are too large, are often for a single baseline. As an example, the interstation vector between Palos Verdes and Buttonwillow (204 km) has a χ^2 of 2.0 in the east-west component and a χ^2 of 0.16 in the north-south component. Noting the location of these stations in Figure 1, it is apparent that this baseline is aligned nearly north-south. The geometry of ground stations and satellites degrades the east-west component (and improves the north-south component), in a way that is not predicted by the formal errors.

The observed short-term precision is a function of our ability to remove error sources associated with satellite orbits, satellite and receiver clocks, and propagation delays; to precisely center the GPS antenna over the monument; and to measure the distance between the antenna base and monument. Precise orbits are not necessarily accurate orbits. Since the accuracy of GPS orbits will influence the accuracy of interstation vectors, we leave that discussion to the next section. Mismeasurement and miscentering of the GPS antenna over the monument are a significant limitation in geodetic measurements of crustal deformation. The constant terms for both horizontal components indicate that centering errors are no greater than 2 mm. It should be noted that over the course of these 11 experiments, no effort was made to send the same field crews and the same equipment to the same sites. Therefore long-term centering errors may be larger, since precise centering may not be accurate centering.

Long-term precision. Although our objective is to summarize long-term precision of interstation vectors from 50 to 450 km in length, it is appropriate to show a few, representative time series of estimates from these networks. We discuss results for two interstation vectors in detail and subsequently tabulate statistics using estimates from all 11 experiments. More time series of interstation vectors will be discussed in the accuracy section.

The baseline from Mojave to the Owens Valley Radio Observatory (OVRO) is frequently used for engineering tests [*Ware et al.*, 1986]. The baseline is approximately 240 km east of the San Andreas fault and is oriented N30°W. The north-south, east-west, and vertical components for this 245-km interstation vector are shown in Figure 5. Mojave-OVRO solutions from the March 1989 experiment are not displayed or used in this calculation of long-term precision because

both sites were tightly constrained to their VLBI values for that experiment. Ignoring this experiment limits the calculation of long-term precision to a temporal span of 14 months, with nine data points measured over four epochs. In the north-south component, the long-term precision is 2 mm. In the east-west component, it is significantly worse, 9 mm. There have been 62 VLBI observations of these sites between 1983 and 1988 [*Ma et al.*, 1990]. VLBI estimates the displacement rate between the sites to be 0.1±2.0 and -2.6±1.4 mm/yr in the north-south and east-west components, respectively. The very precise GPS north-south component is additional evidence that the VLBI measurement

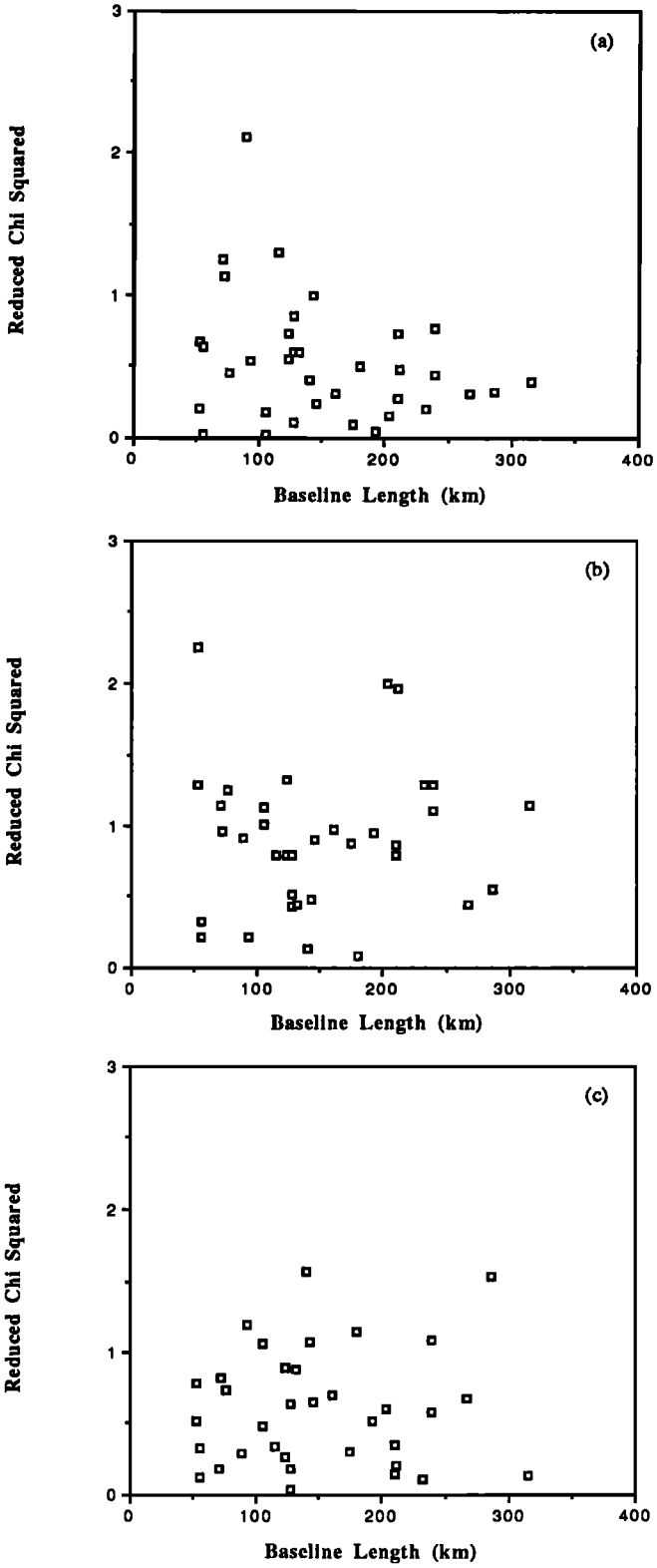

Fig. 4. χ^2 for the baselines shown in Figure 3.

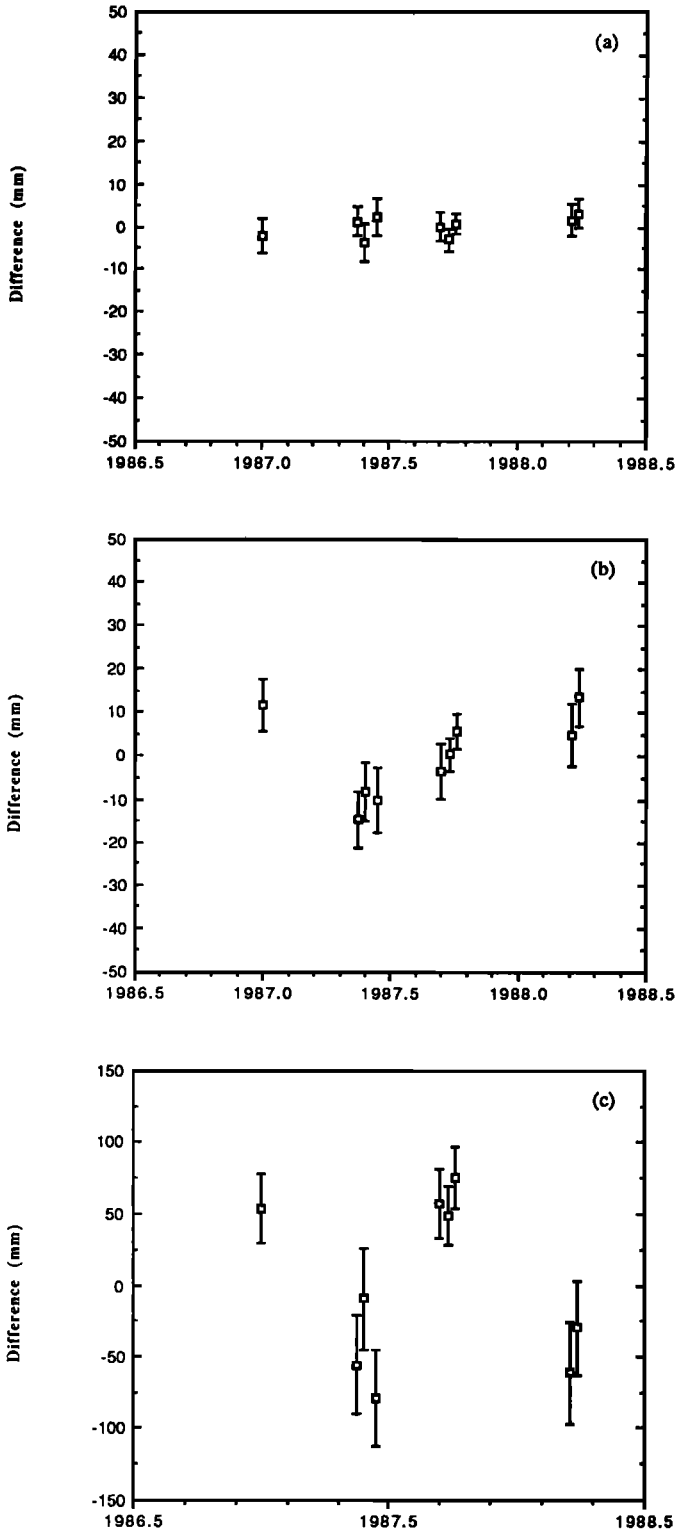

Fig. 5. Change of relative coordinates for the Mojave to OVRO baseline (245 km length), with zero being the mean value. The components shown are defined as in Figure 3, with the coordinate system being centered at the first station.

TABLE 5. Long-Term Precision

Interstation Vector	Length, km	East,[a] mm	χ^2	North,[a] mm	χ^2	Vertical,[b] mm	χ^2	Years	Number of Observations
Lospe-Vandenberg	37	4	2.2	4	2.4	16	0.3	2.2	8
Blancas-Blackhill	53	7	4.0	1	0.1	36	1.6	2.2	8
Clembluf-Brush	54	5	0.7	4	0.8	30	0.8	2.2	8
Lacumbre-Center	55	3	0.8	3	0.8	26	0.7	2.2	11
Madre-Buttonwillow	71	4	1.0	4	3.0	35	1.3	2.2	11
Vandenberg-Madre	76	4	0.9	4	2.0	22	0.6	2.2	10
Madre-Blackhill	76	4	1.0	2	0.4	27	0.8	2.2	11
Blackhill-Vandenberg	91	6	2.2	5	3.1	29	1.1	2.2	13
Palos Verdes-Clembluf	91	10	1.6	5	0.9	39	1.1	2.7	9
Vandenberg Center	101	5	1.4	4	2.5	25	0.8	2.2	16
Palos Verdes-Nicholas	115	8	1.9	4	1.1	29	0.9	2.7	10
Soledad-Clembluf	119	7	1.1	7	3.1	45	1.6	2.7	9
Madre-Center	123	4	1.0	2	0.4	30	1.0	2.2	11
Center-Palos Verdes	127	4	0.6	5	2.2	31	1.1	2.2	16
Buttonwillow-Blackhill	131	3	0.5	5	2.5	32	1.1	2.2	11
Buttonwillow-Blancas	173	6	1.2	5	2.0	42	1.7	2.2	9
Vandenberg-Nicholas	180	6	0.8	9	3.2	26	1.1	2.7	8
Blackhill-Center	181	6	1.5	3	0.6	39	1.5	2.2	16
Palos Verdes-Vandenberg	223	5	0.8	7	3.1	41	1.7	2.2	14
Mojave-Palos Verdes	224	9	1.4	6	1.4	38	1.2	2.2	18
Mojave-Ovro	245	9	1.9	2	0.4	57	4.3	1.2	9
Palos Verdes-Blackhill	286	7	0.9	4	1.0	41	1.6	2.2	12
Ovro-Blackhill	308	13	2.9	5	1.2	34	1.1	2.2	14
Mojave-Vandenberg	351	10	1.5	6	2.4	42	1.8	2.2	18
Mojave-Blackhill	358	6	0.9	4	1.3	46	2.0	2.2	12
Ovro-Vandenberg	363	14	3.0	5	1.2	33	0.9	1.2	11
Ovro-Center	382	14	2.6	5	0.9	47	2.0	2.2	15
				USGS Results[c]					
Mojave-NCMN1	1	2		2		5		2.0	4
10JDG-33JDG	7	6		3		12		3.0	27
10JDG-Joaquin	11	6		5		13		3.0	27
10JDG-Oquin	12	5		4		18		3.0	26
Loma Prieta-Eagle[d]	31	8		4		16		0.9	7
Loma Prieta-Allison[d]	43	8		4		21		0.9	8
Palos Verdes-Vandenberg	223	11		6		40		2.2	6

[a]Weighted RMS about best fitting line, as in equation (3).
[b]Weighted RMS about weighted mean, as in equation (1).
[c]USGS results are taken from *Davis et al.* [1989].
[d]J. Svarc (personal communication, 1990)

of no significant motion in this component is correct. The vertical precision of 57 mm is the worst listed in Table 5.

The long-term precision for the baseline from Vandenberg to Center (located on Santa Cruz Island) is shown in Figure 6. A 101-km baseline oriented NNW, it is considerably shorter than Mojave-OVRO but has been measured almost twice as often, with data spanning 2.2 years. The scatter about the best fit line is 5 and 4 mm for the east-west and north-south components, respectively. The vertical component scatter is 24 mm. All experiments were analyzed with continental-scale fiducial networks, with the exception of the March 1989 data.

The long-term precision statistics are listed in Table 5. For each interstation vector, we computed precision, as defined in the introduction of this section, and the reduced χ^2 statistic. Our criteria for selection of these interstation vectors were that they be estimated during three or more experiments, over at least 1.2 years, with eight or more independent estimates. The long-term precision results have been plotted as a function of baseline length in Figures 7*a*-7*c*. The long-term precision for the north-south component is 4 mm + 0.3 parts in 10^8. In the east-west component, the long-term precision is comparable to the short-term results with a slightly larger constant term, 3.4 mm + 2.0 parts in 10^8. As with our short-term precision results, the vertical component is less precise than either horizontal components and is described by 26 mm + 5 parts in 10^8 of the baseline length. A more careful inspection of Figure 7*c* indicates that long-term vertical precision ranges from 30 to 40 mm, for baselines longer than 50 km, and improves rapidly for smaller values. Thus, for baselines less than 50 km, vertical precision is far better than the constant term of our linear fit, 26 mm, would suggest.

Discussion. We have compiled the long-term precision statistics from *Davis et al.* [1989] and list them in Table 5 along with our interstation vectors. The USGS baselines range from 200 m to 223 km. *Davis et al.* defined precision as the RMS about the best fitting line for both horizontal and vertical components (we compute the RMS about the mean for the vertical component). By including the USGS results, we have a better estimate of GPS precision for baselines less than 450 km in length: 3.4 mm + 1.2 parts in 10^8,

5.2 mm + 2.8 parts in 10^8, 11.7 mm + 13 parts in 10^8 in the north-south, east-west, and vertical components. At 100 km, this would yield subcentimeter horizontal precision, 25 mm in the vertical. Our study overlaps with Davis et al. on one baseline, Palos Verdes to Vandenberg. Our long-term precision of 5, 7, and 41 mm in the north-south, east-west, and vertical only differs appreciably from that of Davis et al. (6, 11, and 40 mm) in the east-west component. We resolved ambiguities on nearly all estimates of this baseline, whereas Davis et al. did not attempt ambiguity resolution. Resolving ambiguities has been shown to improve short-term precision in the east-west component [*Dong and Bock*, 1989; *Blewitt*, 1989], and results from paper 3 indicate that am-

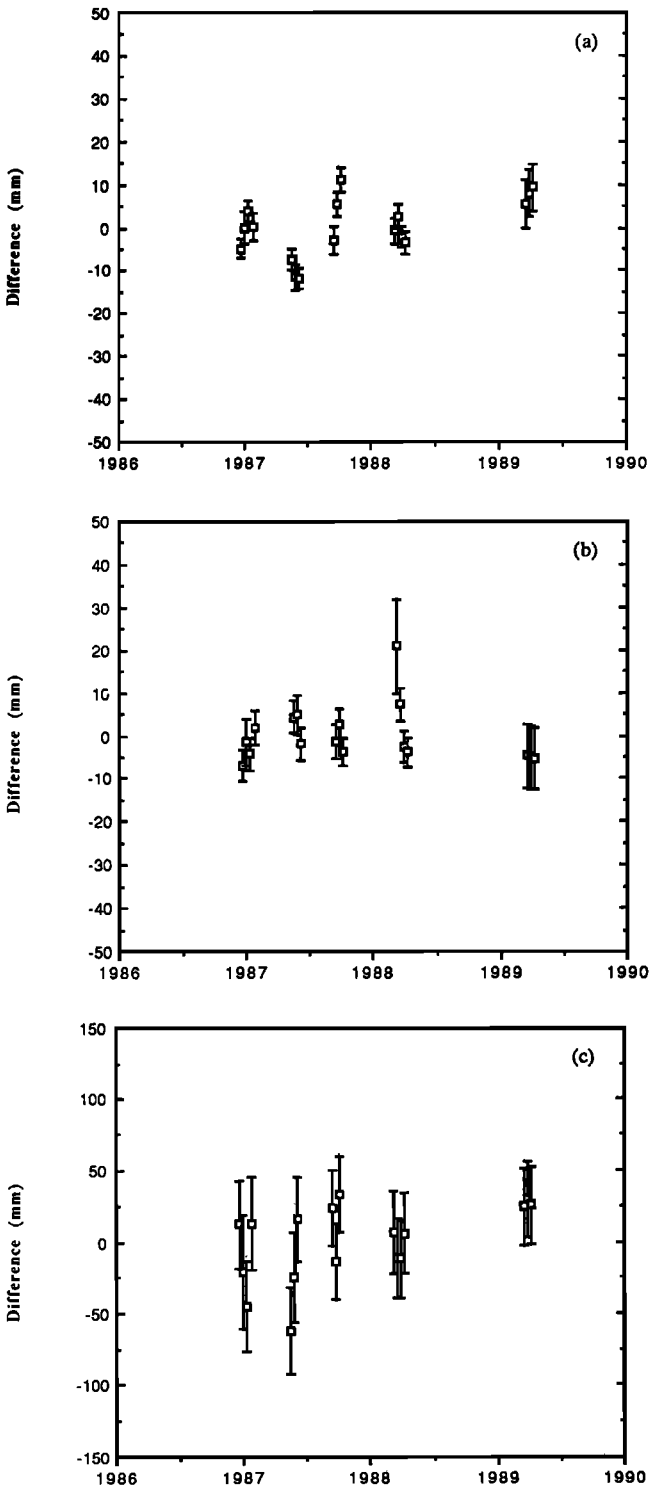

Fig. 6. Change of relative coordinates for the Center to Vandenberg vector (101 km), with zero being the mean value. The components shown are defined as in Figure 3.

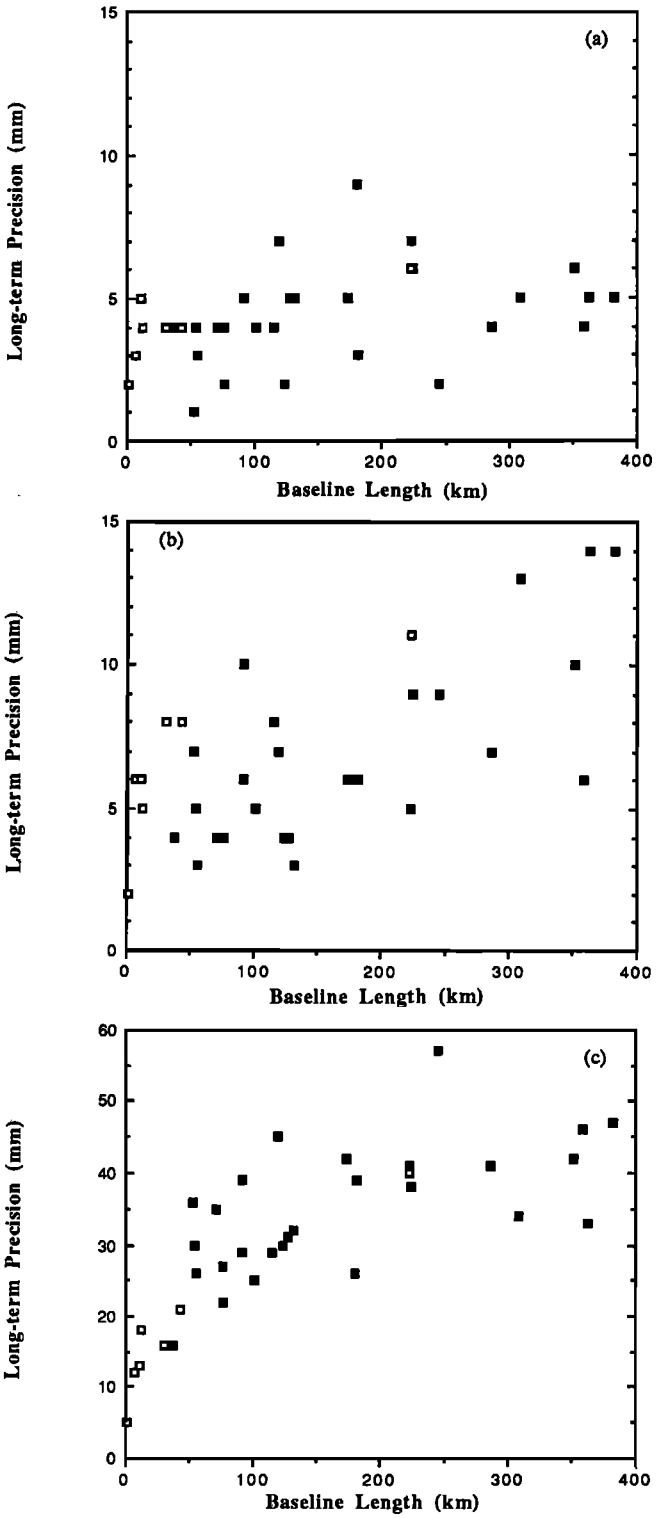

Fig. 7. The solid squares represent the long-term precision determined from experiments described in Table 2. For the horizontal components the precision is defined (equation (3)) as the weighted RMS about the best fitting straight line; for the vertical, by the weighted RMS about the mean (equation (1)). The components are defined as in Figure 3. Also shown are long-term precision determinations (open squares) from *Davis et al.* [1989] for baselines ranging from 200 m to 223 km in length.

biguity resolution improves precision in the long term as well. This may also explain the slightly less precise USGS east-west components for baselines less than 50 km.

Again, we address the question of the validity of our formal errors. In Figures 8*a*-8*c*, we plot χ^2 as a function of baseline length. For the north-south component, our formal errors underestimate the the actual scatter approximately half the time, although χ^2 does not increase with baseline length. For the east-west and vertical components, there is a slight increase of χ^2 with baseline length. Long-term error sources which we think have contributed to the degraded long-term precision are the accuracy of the GPS spacecraft orbit, the ability to resolve carrier phase ambiguities, adequate modeling of the ionosphere and atmosphere, and blunders. Since some of these errors (e.g., orbit accuracy and blunders) have not been accounted for in the formal error, we expect that this has inflated the long-term χ^2 statistic. We discuss each of these error sources in turn.

The orbit accuracy is primarily controlled by the accuracy of the fiducial coordinates, geometry of the fiducial network, and the number of hours of tracking data that were available. Experiments which suffered from failure or absence of continental fiducial sites were, in general, less precise. Additionally, mixing interstation vector estimates computed with different fiducial networks undoubtedly inflates the long-term precision statistic. For the 11 experiments in Table 2, 10 different fiducial networks were used (assuming the three monuments at Mojave to be independent.) Since the purpose of fiducial networks is to provide a consistent reference frame in which to determine crustal deformation rates, their stability is extremely important. The influence of the fiducial network on GPS precision and accuracy is discussed in paper 2. The consistency of our long-term precision with that of *Davis et al.* [1989] leads us to believe that high precision can be achieved with a "single-day" arc, where each day of data yields an independent estimate of satellite orbits and station positions. The precision of single-day arcs on these spatial scales may be dependent on the sophistication of the orbit determination software. For continental-scale (2000-3000 km) baselines, a "multiday" arc solution, as discussed by [*Lichten and Border*, 1987], may be required to achieve comparable precision.

The precision results that we and others (prominently *Dong and Bock* [1989] and *Blewitt* [1989]) have presented were for experiments where a high percentage of carrier phase ambiguities were resolved. The number of hours of tracking influences the confidence statistic used to decide whether the carrier phase ambiguity has been adequately resolved [*Blewitt*, 1989]. In general, we find that ambiguities can be easily resolved with more than an hour of data, with one additional criterion: the interstation spacing should be less than 100 km. In the S88 experiment, the closest spacing of two stations was 223 km. We were only able to resolve 4 of 32 ambiguities. In experiments with closer interstation spacing, e.g., M88b, we were able to resolve 83 of 85 ambiguities in California.

Experiments conducted over a few days do not provide an adequate sampling of tropospheric and ionospheric conditions. This may explain why long-term vertical precision is degraded relative to short-term precision. With the other error sources in these data, it is difficult to isolate the atmospheric and ionospheric contribution. Data that are collected continuously, with a stable fiducial network, will be required to discern the seasonal variations which may be present in these data. Continous GPS networks will also reduce the vertical scatter by eliminating the error associated with centering and measuring the height of the antenna over the monument. Some of the scatter in the vertical component may also be due to human error in translation of field notes into the site vector used in the analysis software.

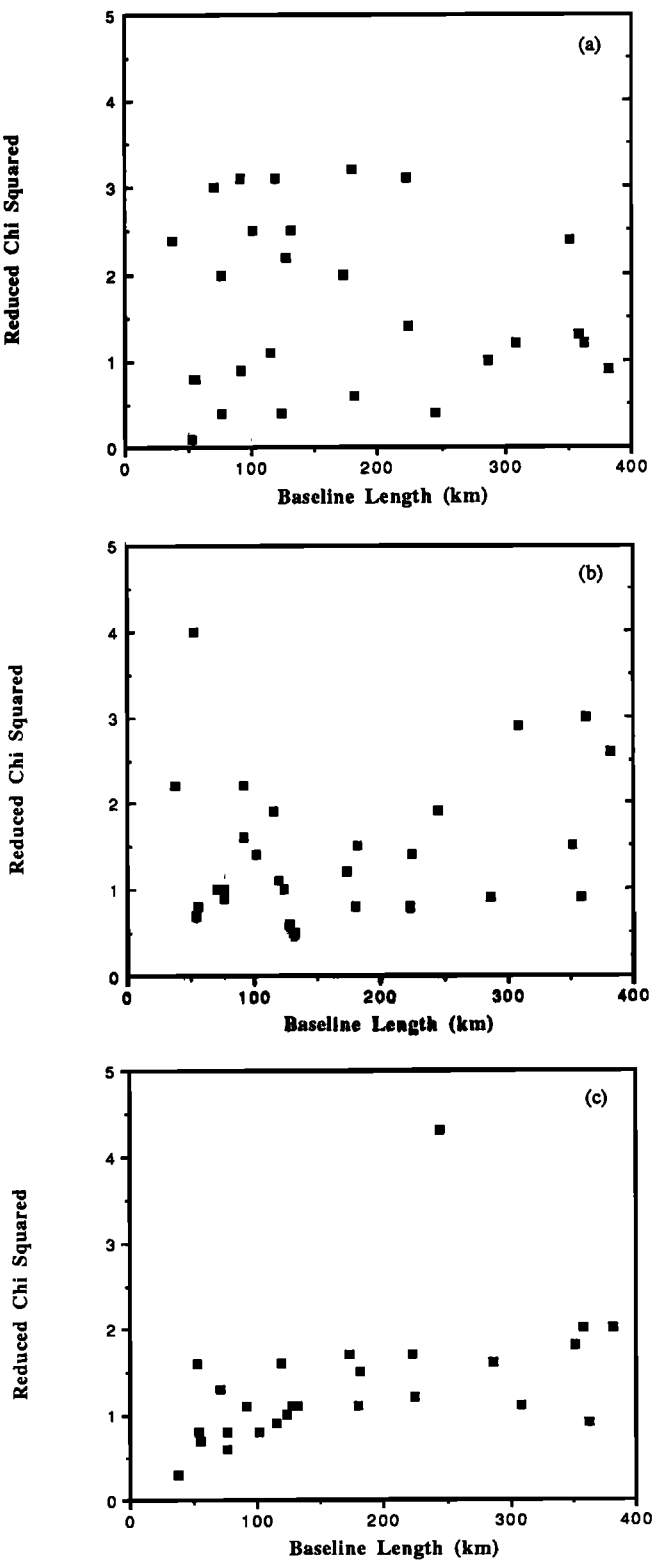

Fig. 8. χ^2 for the baselines shown in Figure 7.

ACCURACY

Introduction

High precision is necessary for, but not indicative of, accuracy. In order to assess accuracy, we must compare GPS vector estimates with vectors determined by an independent measurement system. Comparisons are also useful for identifying systematic errors in GPS, because different techniques presumably have different error sources. VLBI and SLR are two systems available to compare baselines longer than 50 km. No comparisons will be made between GPS and SLR measurements because there are few GPS occupations of SLR monuments in this data set. Unless otherwise noted, the VLBI results are from the 1989 Crustal Dynamics Project Annual Report [*Ma et al.*, 1990] and GLB223, the Goddard site velocity model that was used to determine the GPS fiducial coordinates.

Most estimates of GPS accuracy have been restricted to single epoch agreement with VLBI or SLR [*Dong and Bock*, 1989; *Blewitt*, 1989; *Bock et al.*, 1990], with the exception of work by *Davis et al.* [1989]. Using data from six experiments conducted in southern California, Davis et al. compared GPS and VLBI length estimates of the 223-km baseline between Palos Verdes and Vandenberg. Agreement was within the standard deviations of GPS and VLBI. They also compared line lengths from the Hebgen Lake (9-30 km) and Loma Prieta (30-50 km) networks with the Geodolite, a laser measurement system, with agreement of 1-2 mm at these lengths. At Parkfield, they compared the fault-parallel motion to creep meters and alignment arrays, where rates agreed to within 1-2 mm/yr. While we cannot compare our interstation vectors with as many different kinds of systems, we have concentrated our efforts on the accuracy of "regional" scale baselines. We assess the accuracy of GPS in two modes: agreement of interstation vectors and linear trends.

As with our precision study, we would like to know if accuracy degrades with baseline length. The literature has often referred to agreement with VLBI in terms of parts per baseline length. This is useful if there is a true deterioration of accuracy with baseline length but is inappropriate where errors are not necessarily dependent on baseline length. Certainly, orbit estimation may contribute a baseline dependent error for comparisons at the continental baseline scale, but for baselines shorter than 500 km, there is no evidence to date that the $|GPS - VLBI|$ discrepancy is length dependent.

Comparisons between new and standard measurement systems are essential for validation of the new measurement technique. The difficulty in comparison studies arises in determining the correct rotations which are required to compare vectors which were determined in different reference frames. Even simple comparisons of line lengths determined by EDM and GPS require that a scaling factor be introduced to account for the difference in the speed of light value used in the two data analysis systems. Since GPS vectors are referenced to a VLBI system of fiducial coordinates, GPS and VLBI comparisons are simplified somewhat. A more mundane element of vector comparisons is due to local site surveys. Different systems (VLBI, SLR, GPS) occupy different geodetic monuments at the same geographic location. Generally, these monuments are separated by only several hundred meters, and conventional surveys can be done with an accuracy of a millimeter at these distances. In practice, local surveys introduce uncertainty into the accuracy assessment.

Measurements between the different monuments at these sites (local surveys) are of several types and need to be treated differently. There are conventional surveys, differential GPS determinations, and simple measurements of height above a monument, which we discuss in turn. Conventional surveys have varying levels of redundancy and therefore accuracy. In many cases what are termed survey errors are actually errors in user understanding of the meaning of the coordinate differences coming from ground surveys or blunders in passing along information and not measurement error (W. Strange, personal communication, 1990). The precision of differential GPS surveys on these scales is several millimeters in the horizontals but is twice that in the vertical. *Davis et al.* [1989] reported long-term vertical precision of 5 mm for a 240-m baseline. This is considerably less precise than the best conventional surveys. On the other hand, the accuracy of differential GPS surveys is not well understood or documented. The accuracy of these surveys may be dependent on which GPS receivers were used and which software was used to analyze the measurements. Measurements of height above the geodetic monument are required for both GPS and VLBI. For the TI-4100 GPS receiver, it is assumed that the difference between the L_1 and L_2 phase centers and the antenna base is well known, although discrepancies have been reported (J. Svarc, personal communication, 1990). Likewise, errors in VLBI site vector measurements, for baselines with very few data, will map into a $|GPS - VLBI|$ discrepancy.

As an example of a typical situation in accuracy determinations, Figure 9 illustrates the number of vectors that must be added to compare VLBI and GPS baseline vectors between Mojave and Vandenberg. Terms which are underlined are GPS sites, or antenna phase centers. The numbers refer to the Crustal Dynamics Project site catalog. Two local surveys were required to recover the vector from the main

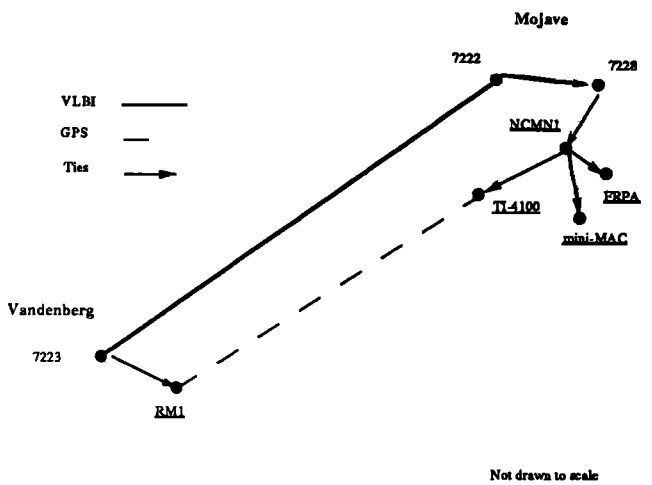

Fig. 9. Cartoon to show the vectors which must be measured to compare GPS and VLBI measurements on a typical baseline. The bold vector between VLBI monuments at Vandenberg and Mojave is 351 km long. The dashed line represents the vector between GPS monuments. GPS monuments/antennae are underlined. Each segment with an arrow represents a local survey which must be conducted to compare GPS and VLBI baseline solutions. This figure is not drawn to scale. Actual survey values are listed in Table 6.

VLBI mark at Mojave to the VLBI reference mark, NCMN1. These surveys were done conventionally. The measurements from NCMN1 to the three permanent antennae which were placed at Mojave between mid-1988 through early 1989 were made with GPS. For completeness, in Table 6 we have listed the relevant local survey information that we have used. In addition to crustal deformation measurement sites in California, we also list local surveys at fiducial sites.

Although it is important to compare interstation vectors at a single epoch (we compare a few vectors measured during the J86 experiment), long-term monitoring of the interstation vector will help to find probable local survey errors. We feel that comparison of rates is ultimately more useful for crustal deformation studies, because the fundamental measurement that we seek is the time rate of change of the vector between two sites. Rate determinations are not immune from local survey errors. If that station is used as a fiducial site in some estimates but not for others, this will influence the computed rate. We discuss only a few interstation vectors in detail.

Results

The data collected in Table 2 were directed toward measuring crustal deformation rates in California. Therefore, comparisons with VLBI are mostly limited to interstation vectors in California. Prominently featured in the available

TABLE 6. GPS-VLBI Local Survey Values

Station 1	Station 2	X, m	Y, m	Z, m	Survey Type	Agency	Reference
			Algonquin Park				
6381	Algonquin (GPS)	92.760	70.280	13.066	conventional	GSC	1
			Mojave				
7222	7288	-323.1130	148.2132	-43.9926	conventional		2
7288	NCMN1	69.6589	-5.9415	35.6147	conventional		2
NCMN1	CIGNET-TI4100	-209.804	120.407	1.836	GPS, NGS[a]	NGS	3
NCMN1	CIGNET-FRPA	-209.7820	120.4134	1.8247	GPS, Bernese[b]	USGS	3
			Owens Valley Radio Observatory				
7207	7853	-820.4891	549.1188	87.1157	conventional		3
7853	7114 (GPS)	-1.2227	-2.2611	-3.6171	conventional		3
			Richmond, Florida				
7219	TIMER 1962	59.722	35.2121	29.920	conventional		3
TIMER 1962	CIGNET-FRPA	0.5483	-3.2420	1.5754	conventional		3
			Westford Observatory				
7209	MICRO	111.191	84.088	43.334	conventional		3
MICRO	CIGNET-TI4100	-84.8933	-45.2645	-12.9246	GPS, NGS	NGS	3
			Vandenberg Air Force Base				
7223	RM1 (GPS)	23.105	-0.9629	17.253	conventional	NGS	1

Compilation of local survey information used, referenced to WGS84. Numbers are associated with the Crustal Dynamics Project VLBI marks. Full listings are given by *Noll* [1988]. For survey types, we distinguish between those done conventionally, and those done with GPS receivers. For GPS surveys, we indicate the software used. All GPS surveys were measured with TI-4100 GPS receivers. If known, the agency which conducted the survey and computed the survey values is listed. References: 1, M. Murray, (personal communication, 1990); 2, J. Ray, (personal communication, 1990); and 3, *Chin* [1988].

[a] *Mader* [1988].

[b] *Beutler et al.* [1987].

TABLE 7. GPS-VLBI Vector Differences

Interstation Vector		Length, km	East, mm	North, mm	Vertical, mm	GPS		VLBI	
						Years	Number of Observations	Years	Number of Observations
Yuma[a]	Monument Peak[a]	208	-10	5	-20	E	2	4.1	8
Mojave	Palos Verdes	224	-15	-12	-80	2.3	18	4.1	5
Mojave	Ovro	245	-8	10	-60	1.2	9	4.3	62
Fort Ord	Vandenberg	256	-10	-15	0	1.2	10	4.2	7
Fort Ord	Ovro	316	5	8	8	1.2	8	4.2	5
Mojave	Vandenberg	351	-15	-13	-50	2.3	18	4.3	89
Ovro	Vandenberg	364	-10	-30	-10	1.2	9	4.2	40
Monument Peak	Vandenberg	430	10	-16	7	E	2	4.0	18

E: single epoch measurement.

[a] See *Noll* [1988] for station description.

data are VLBI sites at Fort Ord, Mojave, OVRO, Vandenberg, and Palos Verdes. GPS and VLBI interstation vector changes will be displayed in a standard form, with the north-south, east-west, and vertical components. Zero is the mean value of the GPS estimates. The solid line in each figure is the VLBI baseline vector component which results from a simultaneous global estimate of site velocities (GLB223). Since this site velocity model was used to compute fiducial locations for the GPS experiments, this is the most appropriate measure of agreement with VLBI. The error bars for the GPS baseline components are one standard deviation. Based on our long-term precision study, these formal errors underestimate the actual uncertainty. The differences between GPS and VLBI for all baselines are listed in Table 7. The interstation vectors compared at more than one epoch which we discuss in greater detail are the vectors between Mojave and Vandenberg, Mojave and Palos Verdes, and OVRO and Fort Ord.

Mojave-Vandenberg-Palos Verdes. In June 1986, the USGS began an effort to regularly measure the interstation vectors between monuments at Mojave, Palos Verdes, and Vandenberg Air Force Base. Due to the commitment of both personnel and receiver time, these are now the most frequently occupied mobile GPS baselines in California longer than 200 km. For Vandenberg and Mojave, there were eight experiments over 33 months, spaced 4-6 months apart. Palos Verdes was occupied simultaneously with Mojave and Vandenberg in seven of those experiments.

Mojave to Vandenberg is the most frequently occupied VLBI baseline in California, with 89 observations between 1983 and 1988. This baseline is long enough to begin to show deterioration in the GPS east component due to poor orbit determination in several of the seven epochs shown, particularly J88 and S88, where we were unable to resolve a large number of the carrier phase ambiguities. Figure 10 displays the GPS vector components from 1986 through 1988. The offset between GPS and VLBI coordinates is 15 mm in the east and 13 mm in the north. The GPS rates derived for the north-south and east-west components of the Vandenberg-Mojave vector are -25.5 ± 2 and 28.9 ± 4 mm/yr, respectively. This agrees within one standard deviation of the VLBI estimates of -28.1 ± 2.0 and 27.6 ± 1.6 mm/yr. The GPS east-west component is significantly noisier than the north-south component, as evidenced by the weighted RMS about the best fitting line: 6 and 10 mm in the north-south and east-west components, respectively. In the vertical component, GPS has a RMS of 41 mm and disagrees with the VLBI mean by 50 mm. The VLBI vertical RMS about the best fitting line is 37 mm.

Palos Verdes was measured by VLBI only five times between 1983 and 1987. We have estimated 18 independent interstation vectors with the GPS data that were collected between 1986 and 1988, as shown in Figure 11. The VLBI and GPS monuments at Palos Verdes are identical. The rates from VLBI are -19 ± 3.7 and 20 ± 3.4 mm/yr in the north-south and east-west components respectively. The GPS rates are similar: -20 ± 2.5 and 28 ± 4 mm/yr. The horizontal components both exhibit an offset of approximately 15 mm. The weighted RMS about the best fitting line for GPS is 8 and 9 mm for the east-west and north-south components. In the vertical component, the precision is less than 50 mm for both VLBI and GPS, but their means disagree by 80 mm. This is the largest difference of eight baselines listed in Table 7.

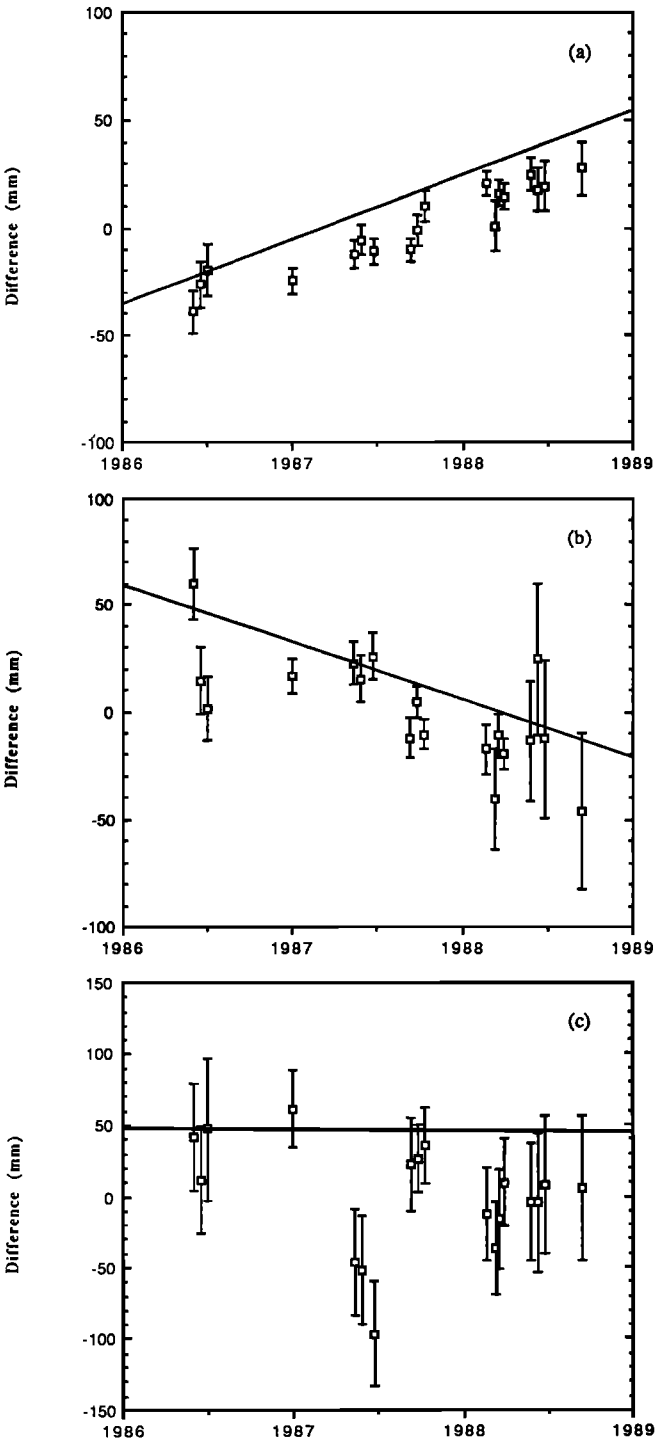

Fig. 10. The points with error bars are the GPS-derived relative coordinates for the Mojave to Vandenberg vector (351 km), taken relative to the mean. The solid line shows the coordinates given by a model fit (GLB223) to the VLBI data. While the agreement in rates is good, there is a persistent offset between the two types of measurement. Components are defined as in Figure 3.

OVRO-Fort Ord. The OVRO-Fort Ord baseline vector is 316 km long and oriented nearly east-west. OVRO requires a conventional survey, but the Fort Ord monument is used by both VLBI and GPS. There have only been three GPS experiments including Fort Ord, over the space of 1.2 years, whereas VLBI experiments span over 4 years. Agreement between GPS and VLBI is shown in Figure 12. Agreement of GPS to VLBI is 5 mm in the east and 10 mm in the

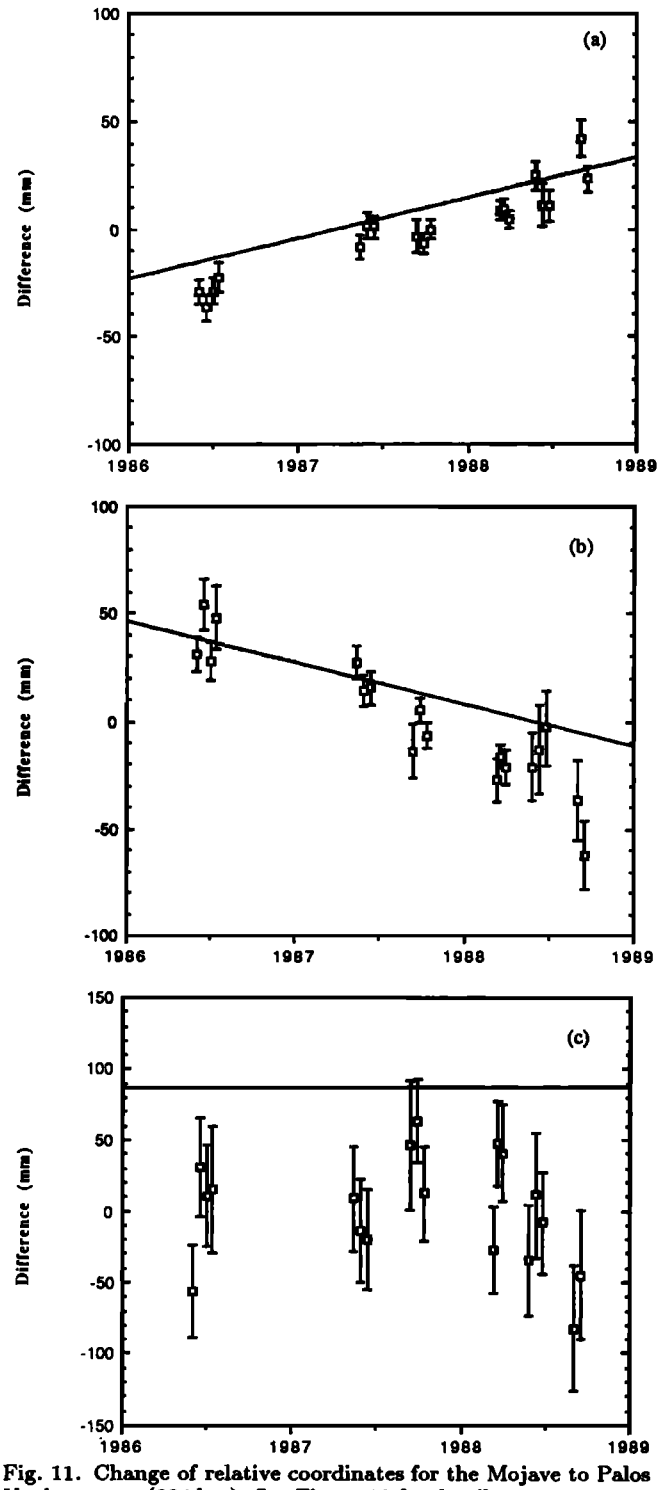

Fig. 11. Change of relative coordinates for the Mojave to Palos Verdes vector (224 km). See Figure 10 for details.

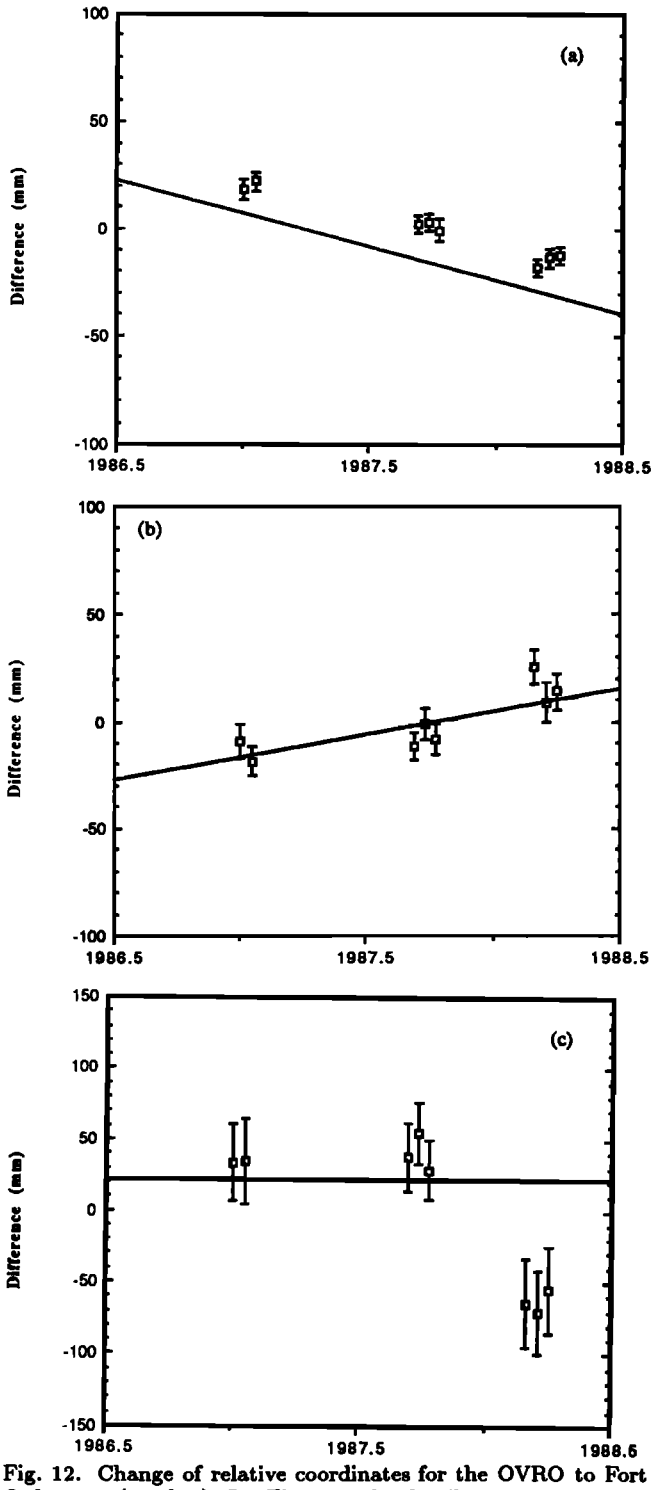

Fig. 12. Change of relative coordinates for the OVRO to Fort Ord vector (316 km). See Figure 10 for details.

north. The vertical agreement is within 20 mm for two experiments and 60 mm for the third. The computed rates for OVRO-Fort Ord agree with VLBI rates within one standard deviation, but the uncertainties on the GPS rate estimates are quite large, due to the short time-span of occupations.

Comparison of Vertical Components

The absolute value of the vertical component difference between GPS and VLBI is shown in Figure 13 as a function of baseline length. The error bar is determined from the weighted RMS about the best fitting line for VLBI and weighted RMS about the mean for GPS. The disagreement is less than 80 mm on baseline vectors ranging from 200 to 430 km. *Dong and Bock* [1989] compared single epoch vertical estimations for the Mojave-OVRO baseline and agreed within 22 mm of the VLBI solution. Results from *Blewitt* [1989] are more comparable to Figure 13, where at a single epoch, the agreement with VLBI was from 5 to 80 mm, measured on 15 baselines ranging from 100 to 1100 km.

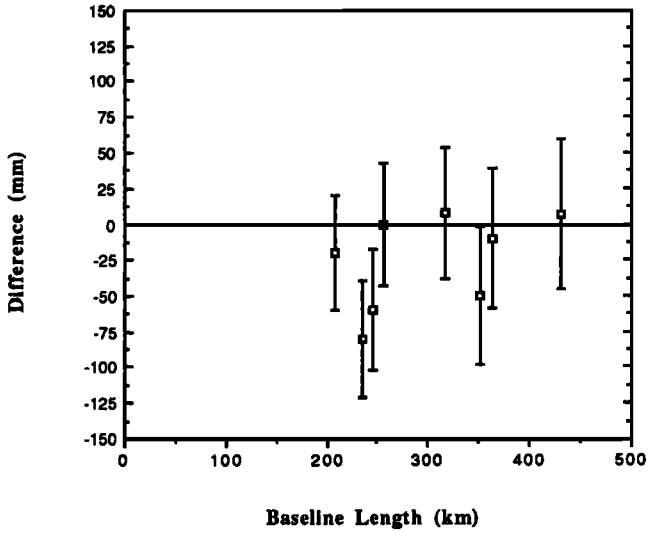

Fig. 13. The GPS-VLBI vertical component difference, plotted as a function of length. The error bar is determined from the weighted RMS about the best fitting line for VLBI [*Ma et al.*, 1990] and weighted RMS about the mean for GPS. More discussion can be found in the text and Table 7.

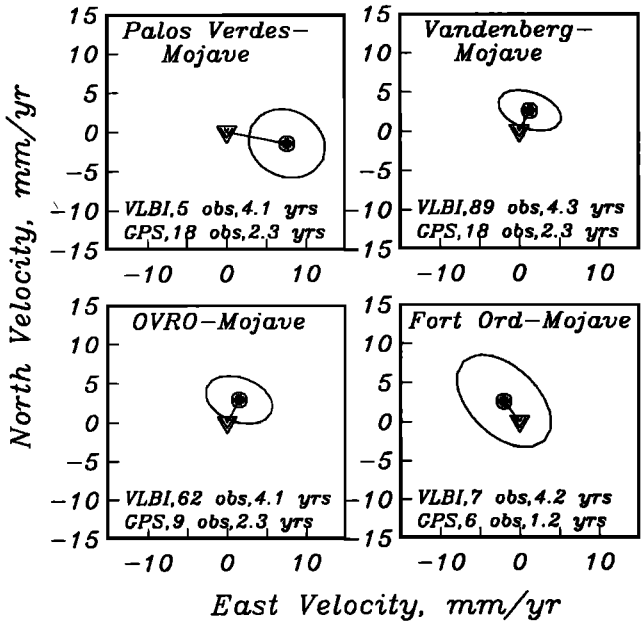

Fig. 14. Difference in vector rates for GPS and VLBI derived motion of Fort Ord, OVRO, Vandenberg, and Palos Verdes relative to Mojave. Zero, shown by the inverted triangle, is the VLBI horizontal rate, and the difference of the GPS rate is shown as a solid circle. Error ellipses are one standard deviation, including both GPS and VLBI. The number of observations and time span of measurements for each baseline are listed.

Comparison of Rates

Finally, we compare rates for four baseline vectors in southern and central California. Figure 14 shows the GPS-VLBI rate difference vector for interstation vectors between Mojave and OVRO, Vandenberg, Palos Verdes, and Fort Ord. The error ellipses were computed from the GPS and VLBI one standard deviations, and then projected onto the horizontal plane. The GPS standard deviations would yield ellipses oriented nearly along the north-south/east-west axes. The addition of the VLBI standard deviations rotates the ellipses slightly, although in general, the GPS standard deviations dominate the error ellipses. The GPS rates for Fort Ord and OVRO are determined from only 1.2 years; those at Palos Verdes and Vandenberg are determined from 2.3 years. The VLBI rates are determined from 4 or more years of data. The only significant difference between GPS and VLBI rates is for the east-west component of Palos Verdes. The vertical rates of deformation for both VLBI and GPS are less than their formal uncertainties.

Discussion

There are several possible reasons that VLBI and GPS vector components disagree, at this level. The differences on some of the interstation vectors listed in Table 7 are suggestive that a single "survey error" may, in fact, be responsible for a large portion of the GPS-VLBI horizontal discrepancy. In order to test this hypothesis, we have taken solutions from the four (D86, S87, M88a and M88b) experiments that include the VLBI sites OVRO, Fort Ord, Mojave, and Vandenberg. These experiments were all analyzed with continental-scale fiducial networks but not necessarily the same ones (as indicated in Table 2). Using the VLBI solutions for these sites at each epoch, we adjusted the GPS interstation vectors and solved for the best fitting "discrepancy" vector at OVRO, Vandenberg, and Mojave. We did not adjust Fort Ord, as the GPS and VLBI monuments are identical. The formal errors from the GPS estimates were used to weight the fit. The results of this calculation are shown in Table 8. The only offsets we consider to be significant are the discrepancies in the north-south and east-west components for Vandenberg, where the best fitting vector is -14 ± 8 and 13 ± 4, and the north-south component at OVRO, 13 ± 2. The

TABLE 8. Estimated Survey Discrepancy Vectors

Experiment	OVRO		Mojave		Vandenberg	
	North	East	North	East	North	East
D86	15±10	-9± 8	5±14	-9± 11	-12±11	-9±9
S87	14± 7	-21± 6	6± 8	-17± 7	-7± 7	-16±6
M88a,b	11 ±8	9± 6	-6± 8	13± 7	-21± 7	-11±7
Weighted mean	13±2	-7±16	1± 7	-3±17	-14±8	-13±4

All values are in millimeters.

latter is particularly surprising, given the energy which was expended to remeasure the line between Mojave and OVRO in the "MOTIES" experiment (J. Ray, personal communication, 1989). The result is consistent with the observed discrepancy between Mojave and OVRO of 10 mm. Likewise, the discrepancy at Vandenberg would explain the long-term discrepancy between Mojave and Vandenberg and would be sufficient to create the largest discrepancy on these regional baselines, between OVRO and Vandenberg

Another reason for horizontal component discrepancies is the robustness of the solution for the vector, either from GPS or VLBI. Both systems will reduce the uncertainty in the interstation vector with additional data. Some vectors (such as OVRO-Fort Ord) are measured by VLBI once per year, whereas the VLBI Mojave-Vandenberg vector is based on 89 measurements. Both Mojave and Vandenberg are fixed VLBI antennas, whereas Fort Ord is a mobile VLBI site. The interstation vectors between fixed antennas (which generally are measured more often) are more precisely known than those between mobile antennas.

The vertical component discrepancies, while troubling for some baseline vectors, are based on very few data points. We assumed that the GPS phase center, which varies with elevation angle to the GPS satellite, averaged to some mean value. This phase center variation may in fact introduce a systematic bias, which could introduce the offset we see between GPS and VLBI. GPS vertical components are particularly sensitive to poor fiducial networks (see paper 2). Another possible source of vertical discrepancies is differences due to the estimation technique used to determine propagation delays of the atmosphere. We discuss this further in paper 3.

The agreement between GPS and VLBI rates in all components is extremely encouraging, particularly considering the short time span of GPS data collection. We expect that the rate agreement will continue to improve as we collect more data and eliminate systematic errors.

CONCLUSIONS

We have analyzed nearly 3 years of GPS data collected in southern and central California between 1986 and 1989. On time scales of a few days, horizontal precision is 2 mm, with an additional length dependence of 0.6 and 1.3 parts in 10^8 for the north-south and east-west components, respectively. Short-term precision in the vertical is length independent, with a mean value of 17 mm. Horizontal precision determined over several years, where we have included recent precision estimates from the USGS [*Davis et al.*, 1989], has a constant bias of 5 mm, with a length dependence of 1 and 3 parts in 10^8 for the north-south and east-west components, respectively. These measurements were made when the GPS constellation was preferentially aligned north-south. Presumably, the precision of future GPS measurements will show less dependence on the direction of the interstation vector. Vertical measurements are much less precise than horizontal measurements, 11.7 mm + 13 parts in 10^8.

Accuracy (defined by agreement of horizontal components with those found from VLBI) is 5-30 mm for baselines from 200 to 430 km long. The pattern of these discrepancies is consistent with a survey discrepancy at two VLBI sites in California, Vandenberg and OVRO. For interstation vectors that do not include these sites, agreement of horizontal components is approximately 10 mm. The vertical discrepancies between VLBI and GPS are much larger, ranging from 0 to 80 mm. There does not seem to be a systematic bias between the two systems, which in any case is unlikely because VLBI defines the orientation and scale of the GPS reference system. For making crustal deformation measurements, the most important comparison may be between the vector rates determined by the two systems. The GPS-determined vector rates agree well with those determined from VLBI measurements.

These results confirm the study of *Davis et al.* [1989], which found that precision and accuracy (in rates) was subcentimeter on these spatial scales. In turn, this confirms that GPS geodetic measurements are appropriate for crustal deformation experiments, where signals range from several millimeters to hundreds of millimeters per year. This precision and accuracy may not, of course always be achieved, and there are reasons why the data set we have studied may be better than most. Although we cannot prove this assertion, we feel that one of the most important factors in repeating high-accuracy GPS measurements is keeping as many factors common to all experiments as possible. Although the tracking data for the different experiments have not been homogeneous, most other factors were: the same GPS receiver and data analysis software were used; the same type of GPS antenna was used at nearly all stations; and the same GPS satellites (which followed nearly the same apparent sky paths) were available. The challenge remains for the geodetic community to successfully mix different receivers, antennas, block I and block II GPS satellites, and analysis software and to retain the high precision and accuracy achieved with the block I GPS constellation.

Acknowledgments. Much of the GPS data used in this paper were collected as part of a collaborative project to measure crustal deformation in central and southern California by the Scripps Institution of Oceanography, California Insititute of Technology, University of California, Los Angeles, and Massachusetts Insitute of Technology. We are particularly indebted to dozens of graduate students who contributed their time to this effort. The principal investigators, Dave Jackson, Bob King, Tom Jordan, and Brad Hager, were instrumental in making these experiments possible. The scope of this study would not have been possible without the cooperation and participation of the NGS and USGS, which were conducting their own surveys in the region. We thank Bill Strange and Will Prescott for supervising the collection of high-quality GPS data in California. Tracking data were provided by CIGNET. We thank Jerry Mader, Miranda Chin, and Linda Nussear for helping us acquire these data. Additional data and receivers were provided by JPL, CIGNET, DMA, PMTC, and the Geodetic Squadron of Canada. Logistical (James Stowell) and archival (Judah Levine) support was provided by UNAVCO. One of the authors (K.M.L.) benefitted from numerous conversations with Jim Davis, Geoff Blewitt, Will Prescott, and Steve Lichten. K.M.L. would also like to thank Mark Murray, Frank Webb, Kurt Feigl, Jeff Freymueller, Jerry Svarc, and Shawn Larsen for helpful discussions on GPS data analysis techniques. Computing facilities and the GIPSY software were provided by the Jet Propulsion Laboratory. We particularly thank Tom Yunck and Tim Dixon and their groups for supporting this work. Written reviews by Jim Davis, Bill Strange, Steve Lichten, and George Born improved the quality and scope of this paper. The data collection was funded (at UCSD) by NSF EAR-8618165. This research was supported by a NASA Graduate Student Research Fellowship awarded to K.M.L. at Scripps Institution of Oceanography. The writing and publication were completed at the Colorado Center for Astrodynamics Research and supported by ONR N0001490J2010.

REFERENCES

Beutler, G., I. Bauersima, W. Gurtner, M. Rothacher, T. Schildknecht, G. L. Mader, and M.D. Abell, Evaluation of the 1984 Alaska Global Positioning System campaign with the Bernese GPS software, *J. Geophys. Res., 92,* 1295-1303, 1987.

Bevington, P., *Data Reduction and Error Analysis for the Physical Sciences*, McGraw-Hill, New York, 1969.

Blewitt, G., Carrier phase ambiguity resolution for the Global Positioning System applied to geodetic baselines up to 2000 km, *J. Geophys. Res., 94,* 10,187-10,203, 1989.

Blewitt, G., An automatic editing algorithm for GPS data, *Geophys. Res. Lett., 17,* 199-202, 1990.

Bock, Y., R., I. Abbot, C.C. Counselman III, and R.W. King, A demonstration of one to two parts in 10^7 accuracy using GPS, *Bull. Geod., 60,* 241-254, 1986.

Chin, M., CIGNET report, GPS bulletin, Global Positioning Subcommission of Comm. VIII, Int. Coord. of Space Technol. for Geod. and Geodyn., Natl. Geod. Surv., Rockville, Md., 1988.

Christodoulidis, D.C., D.E. Smith, R. Kolenkiewicz, S.M. Klosko, S.M. Torrence, and P.J. Dunn, Observing tectonic plate motions and deformations from satellite laser ranging, *J. Geophys. Res., 90,* 9249- 9263, 1985.

Clark, T.A., D. Gordon, W. E. Himwich, C. Ma, A. Mallama, and J. W. Ryan, Determination of relative site motions in the western United States using Mark III very long baseline interferometry, *J. Geophys. Res., 92,* 12,741-12,750, 1987.

Davis, J.L., W.H. Prescott, J. Svarc, and K. Wendt, Assessment of Global Positioning System measurements for studies of crustal deformation, *J. Geophys. Res., 94,* 13,635-13,650, 1989.

Dong, D., and Y. Bock, Global Positioning System network analysis with phase ambiguity resolution applied to crustal deformation studies in California, *J. Geophys. Res., 94,* 3949-3966, 1989.

Hayford, J. F., and A. L. Baldwin, Geodetic measurements of earth movements, in *The California Earthquake of April 18, 1906*, edited by A. L. Lawson, pp. 114-145, Carnegie Institution, Washington D.C., 1908.

Henson, D. J., E. A. Collier, and K. R. Schneider, Geodetic applications of the Texas Instruments TI 4100 GPS navigator, paper presented at the 1st International Symposium on Precise Positioning with the Global Positioning System, U.S. Dep. of Commer., Rockville, Md., April 15-19, 1985.

Herring, T. A., et al., Geodesy by radio interferometry: evidence for contemporary plate motion, *J. Geophys. Res., 91,* 8341-8347, 1986.

Larson, K. M., Precision, accuracy, and tectonics from the Global Positioning System, doctoral dissertation, Univ. of Calif., San Diego, 1990.

Larson, K. M., F.H. Webb, and D.C. Agnew, Application of the Global Positioning System to crustal deformation measurements. 2. The influence of orbit determination errors, *J. Geophys. Res.*, this issue.

Lichten, S.M., and J.S. Border, Strategies for high precision GPS orbit determination, *J. Geophys. Res., 92,* 12,751-12,762, 1987.

Lichten, S.M., High accuracy Global Positioning System orbit determination: Progress and prospects, in *Proceedings of the General Meeting of the I.A.G., August 3-12, 1989, Edinburgh, Scotland, GPS and Other Radio Tracking Systems*, edited by Y. Bock and N. Leppard, pp. 40-52, Springer-Verlag, New York, 1990.

Ma, C., J.W. Ryan, and D. Caprette, Crustal Dynamics Project data analysis-1988, *NASA Tech. Memo., TM-100723,* 1989.

Mader, G.L., GPS Data Processing Program Documentation, Geodetic Research and Development Lab, NGS Division, Rockville, MD, August, 1988.

Noll, C., Crustal Dynamics Project: Catalogue of site information, *NASA Ref. Publ., 1198,* 1988.

Rueger, J. M., *Electronic Distance Measurement: An Introduction*, Springer-Verlag, New York, 1990.

Savage, J. C., Strain accumulation in the western United States, *Ann. Rev. Earth Planet. Sci., 11,* 11-43, 1983.

Savage, J.C., and W.H. Prescott, Precision of Geodolite distance measurements for determining fault movements, *J. Geophys. Res., 78,* 6001-6007, 1973.

Smith, D.E., et al., Tectonic motion and deformation from satellite laser ranging to LAGEOS, *J. Geophys. Res., 95,* 22,013-22,042, 1990.

Sovers, O.J., and J. S. Border, Observation model and parameter partials for the JPL geodetic GPS modeling software GPSOMC, *JPL Publ., 87-21,* 1988.

Stephens, S., GIPSY frontend user's guide, *JPL Publ., D-3918,* 1986.

Tralli, D. M., T. H. Dixon, and S. Stephens, The effect of wet tropospheric path delays on estimation of geodetic baselines in the Gulf of California using the Global Positioning System, *J. Geophys. Res., 93,* 6545-6557, 1988.

Ware, R. H., C. Rocken, K. J. Hurst, and G. W. Rosborough, Determination of the OVRO-Mojave baseline during the spring 1985 GPS test, in *Proceedings of the Fourth International Geodetic Symposium on Satellite Positioning*, vol. 2, pp. 1089-1101, Natl. Geod. Surv., Rockville, Md., 1986.

D. C. Agnew, Institute of Geophysics and Planetary Physics, Scripps Institution of Oceanography, La Jolla, CA 92093.

K. M. Larson, Colorado Center for Astrodynamics Research, University of Colorado Boulder, CO 80309-0431.

(Received August 5, 1990;
revised May 6, 1991;
accepted May 6, 1991)